Chapter-3

Development of biodegradable film from modified starch, protein and their blends

3.1. Introduction

The increasing concern about pollution caused by non-biodegradable items shows the principal driving agents for forming bio-based packaging materials with enhanced qualities for sustainability. The efficient substitution of similar materials with biodegradable polymers derived from degraded sources (i.e., biopolymers) could reduce the severe environmental effect of packaged products (Kumar et al., 2023). Given its natural abundance, starch is economically priced in the market, especially when compared to other synthetic and bio-based polymers. It can be produced by plants through photosynthesis from carbon dioxide and water (Hoque et al., 2013; Liu et al., 2022). Starch, being a biodegradable polysaccharide produced in abundance at low cost and exhibiting thermoplasticity, appears to be an excellent raw material for biodegradable polymers (Jiang et al., 2020). India, as the second-largest potato producer globally, contributes about 11.26% of the total potato production worldwide, approximately 34.4 million MT (Jagadeesan et al., 2020). Potato starch (PS) is considered as most promising carbohydrate for food packaging applications (Niu et al., 2021). Its starch granules are relatively big (25–100 μm), occurring in a B-type crystalline structure (Jagadeesan et al., 2020). PS comprises the characteristics of high viscosity, high paste clarity, low tendency to retrograde, low pasting temperature, and easy expansion of starch granules (Zhang et al., 2018; Li et al., 2021). It contains a relatively higher number of phosphorous groups compared to other sources of starches (Zhang et al., 2018). PS also acquires the required thermoplastic trait desirable in forming bio-film (Varatharajan, 2010). Although these unique characteristics together make PS an excellent choice as a functional biomaterial in the case of food and polymer science (Singh et al., 2008), PS usage containing 80% large macromolecules of branched amylopectin shows several limitations for packaging, such as poor mechanical strength, poor moisture sensitivity, greater dissolving temperature and poor solubility (Menzel, 2014; Niranjana and Prasantha, 2018).

Protein films demonstrate exceptional gas, water vapor, and mechanical properties, while polysaccharide films exhibit excellent gas permeability (Roy et al., 2024). Observations indicate that proteins offer better mechanical properties than polysaccharides, providing excellent barrier properties for aroma and oil. However, compared to composite polymers, proteins exhibit poorer mechanical strength and higher water vapor permeability (Kandasamy et al., 2021). Caseins make excellent choices for creating biodegradable and active films because they have several advantageous properties: they are nutritionally rich, can effectively form emulsions, dissolve well in water, and remain stable across different pH levels (Mishra et al., 2022). However, casein is moisture-sensitive, limiting its applications when exposed to high humidity. Additionally, starch-based films' hydrophilicity leads to water solubility and poor water barrier characteristics (Hassan et al., 2018; Kocira et al., 2021). Proteins and starch, serving as potent biopolymers, thereby are utilized to create biodegradable and edible food packaging. Compared to the creation of new macromolecules, blending is more cost-effective and simpler (Roy et al., 2024). It holds immense potential in improving the viability of biopolymers. Composite films combining proteins and polysaccharides can however overcome individual material limitations, enhancing mechanical and barrier properties (Kumar et al., 2023). These films amalgamate the advantages of each component, resulting in excellent mechanical and barrier characteristics (Basumatary et al., 2022). However, proteins and starches require modifications to mimic traditional petroleum-based materials' mechanical and barrier properties when used in films or coatings. This chapter thus investigates the potential of PS and casein along with their blends as sustainable alternatives to synthetic packaging materials. It examines the effects of various modifications (heat-moisture treatment (HMT) and annealing (ANN) for PS, US (ultrasound), and AC (autoclave) for casein) on the mechanical, barrier and physicochemical characteristics of these biopolymers along with their obtained films.

3.2. Materials and methods

3.2.1. Collection of samples

Solanum tuberosum L was purchased from a nearby farm, close to Tezpur University in Assam, India. Additionally, casein (CN, purity >90%) was purchased through Zenith India Pvt. Ltd., India.

3.2.2. Starch isolation

Fresh *S. tuberosum* L tubers were harvested from a farm near Tezpur University. These tubers were peeled, grated using a fruits and vegetable grater, and washed under running water. Starch extraction followed a modified version of the Sit et al. (2013) protocol. The grated pieces underwent 1-2 min of processing in a high-speed laboratory blender (Philips HL 1632, India). The resulting slurry was diluted with distilled water (DW) at a 1:10 ratio. This suspension was first passed through a 150 μm mesh sieve and then filtered using a double-fold muslin cloth. The filtrate was allowed to sediment for 2-3 h. After discarding the supernatant, the sediment underwent two additional DW cleaning cycles. The final sediment was dried in an oven at 45°C for 24 h. The dried starch was then crushed and passed through a 100μ mesh sieve to obtain the final product.

3.2.3. Modification of PS through annealing (ANN)

A modified version of Chung et al. (2009) protocol was used for the annealing (ANN) treatment. Dry starch samples were placed in glass beakers and combined with distilled water at a 1:2 starch-to-water ratio. The sealed samples were heated to 60°C in a water bath for 24 h. The annealed starches were then repeatedly washed with DW, filtered, and air-dried to achieve a consistent 10% moisture content.

3.2.4. Modification of PS through heat-moisture treatment (HMT)

Heat-moisture treatment (HMT) followed a modified version of Pranoto et al. (2014) methodology. Native potato starch (NPS) underwent HMT modification by adjusting sample moisture content to 20% and equilibrating at 5°C for 15 h. These samples were then heated at 110°C for 8 hours in an oven. To prevent further gelatinization, the samples were immediately cooled upon removal and then dried overnight at 50°C in a drying oven. The HMT-modified starches were cooled to ambient temperature before storage for subsequent analysis.

3.2.5. Modification of casein by ultrasound (US)

The modification of the casein was performed in an ultrasonic processor (Ultrasonic Homogenizer Model U500 TAKASHI) employing a 6 mm-diameter probe and a fixed 35 kHz frequency according to Biswas and Sit (2020). For modification, 10 g of

casein powder was combined with 100 mL of DW in a 250 mL beaker and retained for ultrasonic modification with variable ultrasound duration and intensity. Two treatment durations (15 and 30 min) and ultrasound power (180 W) with a frequency of 35 kHz were applied. After ultrasonication, casein was isolated by centrifugation at 7800×g and the precipitated portion was recovered after 15 min. The precipitated casein was then kept for drying at 40°C for 24 h to prevent denaturing of the modified casein during drying. For further testing, the dried casein powder was stored in airtight containers.

3.2.6. Modification of casein by autoclave (AC)

According to the methodology of Wu et al. (1999), modification of casein using an AC has been carried out. 10 g casein powder was weighed into glass containers and sealed. AC was carried out using an autoclave performed at various durations (15 and 30 min) at 121℃ and 15 psi pressure. After autoclaving, obtained casein was held for 24 h at 40℃ for drying. For further testing, the dried casein powder was stored inside airtight containers.

3.2.7. Preparation of PS-based films

The preparation of potato starch (PS) films, including Native PS films (NPSF), Annealed films (ANNF), and Heat-moisture treated films (HMTF), followed the solution casting methodology described by Badwaik et al. (2014). The process began by combining 5 g (dry basis) of each starch variety with 100 mL DW in a 250 mL conical flask. To reduce brittleness, the solution was modified with 2 mL glycerol (equivalent to 40 mL per 100 g solid matter). Complete gelatinization was achieved by maintaining the mixture at 90°C for 30 min with constant agitation at 300 rpm using a hot plate magnetic stirrer. Subsequently, the mixture was cooled to 40°C until air bubble formation ceased. The gelatinized suspension (40 mL) was transferred to level sterile petri dishes (150 mm × 150 mm × 10 mm) and underwent oven drying at 40°C for 15 h. After formation, the films were removed from the petri dishes and conditioned in an incubator at 65% RH and 25°C. Prior to analysis, the films were stored for a minimum of one week in a desiccator containing saturated silica powder (56% RH) at 30°C. Various parameters as discussed in Section 3.2.12 were then measured to characterize the film properties.

3.2.8. Preparation of casein-based films

For the casein-based films, the preparation method followed Cortes-Rodriguez et al. (2020). The process involved dissolving casein powder in 0.2% weight aqueous NaOH at 80°C for 3 hours, using a three-necked round bottom flask equipped with a thermometer. Glycerol was incorporated into the casein solution at 80°C with 10 min of mixing. Film formation involved casting 50 g of the prepared solution onto level sterile petri dishes (150 mm diameter, 10 mm thickness) and drying at 40°C in a hot air oven for 15 h. The resulting films were stored in dry conditions until testing, followed by conditioning in a desiccator with saturated silica powder (56% RH) at 30°C for at least one week before evaluation. The final products - native casein films (NCF), ultrasound-treated films (UTF), and autoclave-treated films (ATF) - underwent various property assessments.

3.2.9. Preparation of film by using different blends of PS (PS) and casein

Table 3.1 depicts the formulation process for the PS and casein blended films. Films were created using blends of PS and casein, following the methodology outlined by Basiak et al. (2017). The suspensions, containing different ratios of PS to casein as detailed in **Table 3.1**, were prepared via the solution casting method. The process involved preparing PS and casein films by agitating them in a 0.2% NaOH solution at 80°C for 3 h in a round-bottom flask equipped with a thermometer to ensure thorough mixing. Glycerol was added at a rate of 40 mL/100 g (0.5 g g solids^{-1}) as a plasticizer and mixed evenly. The resulting blended suspensions (40 mL each) were cast onto leveled sterile Petri dishes (150 mm diameter and 10 mm height) and dried in a hot air oven at 40°C for 15 h to produce PS-casein-based blended films. Subsequently, the films were stored under dry conditions until testing. Before testing, the conditioned films were placed in a desiccator with saturated silica powder (56 % RH) at 30°C for a minimum of one week. Post this conditioning, the films were evaluated for various characteristics associated with biofilm formation. The formulation of the film used for film preparation is shown in **Table 3.1.**

Table 3.1. Composition used for formulation of potato starch (PS) and casein-based blended film

Proportions	PS (% w/v)	Casein (% w/v)	Glycerol (mL)
30:70	30	70	40
40:60	40	60	40
50:50	50	50	40
60:40	60	40	40
70:30	70	30	40

3.2.10. Properties of starches

3.2.10.1. Swelling power (SP) and solubility (S)

To obtain swelling power (SP) and solubility (S) of the PS (native and modified), the method of Lee and Yoo, (2011) was followed. One percent starch solution was prepared and cooked in a water bath at 90°C for 30 min with steady stirring and then cooled. The suspension was centrifuged for 10 min at 3200 rpm. After centrifugation, the sediment part was measured for SP value using equation **(3.1)**. The supernatant was poured out in a pre-weighed petri dish which was then dried at 110℃ until achieving a constant weight for quantification of the soluble fraction, weighing, and calculation of solubility (S) value. The solubility was obtained using equation **(3.2)**.

The swelling power (SP) and solubility (S) (%) were calculated by the formulas below:

$$\text{Swelling Power (g g}^{-1}) = \frac{\text{Weight of swollen granules} \times 100}{\text{Weight of sample} - \text{Weight of dissolved starch}} \quad (3.1)$$

$$\% \text{ Solubility} = \frac{\text{Weight of dried starch in Petri dish}}{\text{Sample weight}} \times 100 \quad (3.2)$$

3.2.10.2. Color

Color attributes of the 5% PS paste (native along with modified) prepared through gelatinization were determined by colorimeter (Ultrascan VIS, Hunterlab, USA). L*, a*, and b* values were noted. Values were represented by expressing parameters of L* (lightness), a* (redness), and b* (yellowness). The degree of whiteness (DW) was calculated using equation **(3.3)**, respectively.

$$DW = \left[100 - \sqrt{\{(100 - L)^2 + a^2 + b^2\}}\right] \quad (3.3)$$

3.2.10.3. Freeze-thaw stability

The methodology of Brahma and Sit, (2020) was applied to determine the freeze-thaw stability of PS pastes. A total of 5 freeze-thaw cycles were evaluated in the present study. Starch (5% w/v dry basis) was cooked at 95°C for half an hour under steady mild shaking conditions and was further cooled to room temperature. After cooling, the paste (15g) was weighed into previously weighed centrifuge tubes. The starch pastes were then put through subsequent freeze-thaw cycles by freezing at -20°C for 22 h followed by thawing at 30°C for 2 h and then centrifuged at 8000 × g for 10 mins after each cycle for 5 days. The supernatant removed from the gel was measured, and the percent syneresis was determined by the weight of exudates to the weight of the paste equation **(3.4)**.

$$\% \text{ Syneresis} = \frac{\text{Water separated (g)}}{\text{Total sample weight}} \times 100 \quad (3.4)$$

3.2.10.4. Pasting properties

The pasting characteristics of PS pastes were measured using a Rapid Visco Analyser (RVA; Techmaster, Newport Scientific Pty. Ltd., Australia following the procedure of Rizwana and Hazarika, (2022). 3g starch was weighed, and 27 mL of distilled water was added to it. The starch slurry was prepared and then put directly in the RVA-4 number canister. The sample was held at 50°C for a min, heated until 95°C at the rate of 12°C/min within 3.75 min, and thereafter, held at 95º C for about 2.5 min. The sample was further cooled down to 50°C at the same rate of 12°C/min. The rotating motion of the stirrer was set at 960 rpm for 10 s and was subsequently changed to 160 rpm for the rest of the analysis. Pasting temperature (PT), peak viscosity (PV), final viscosity (FV), hold viscosity (HV), breakdown viscosity (BV), and setback viscosity (SV) were determined. Viscosity was represented in centipoise (cP).

3.2.10.5. Rheological properties

The rheological characteristics of PS pastes (both native and modified) were evaluated using an Anton Paar MCR 72 rheometer with a parallel plate configuration (25 mm diameter, 1 mm gap), following the methodology of Shanthilal and Bhattacharya

(2015). The preparation involved creating a 5% w/v starch dispersion in DW, heating it at 95°C for 30 min in a water bath, cooling it to 25°C, and transferring it to the rheometer plate. Frequency sweep measurements ranged from 0.1 to 10 Hz. Both steady and dynamic shear conditions were examined, with shear rates ranging from 0 to 500 s^{-1}. Dynamic rheological parameters measured included storage modulus (G′), loss modulus (G″), complex viscosity (η*), and phase shift angle (δ) across the frequency range. The relationship between viscosity (Pa.s) and shear rate (s^{-1}) was plotted.

3.2.11. Properties of Casein

3.2.11.1. Protein solubility

The protein solubility of casein (native along with modified) was analyzed by Butt and Rizwana (2010) procedure. 0.25 g casein powder was homogenized in 20 mL 0.1 M NaCl solution which was thereafter maintained at 7.0 pH holding for 1 h. Centrifugation for 30 min was done at 10,000×g. The amount of nitrogen content of the soluble fraction was calculated using the Kjeldhal procedure. Using the following equation **(3.5)**, solubility was determined as the ratio of total nitrogen in the original sample to nitrogen in the soluble fraction.

$$\text{Solubility} = \frac{\text{Protein content in the supernatant}}{\text{Total protein content in the sample}} \text{ x } 100 \qquad (3.5)$$

3.2.11.2. Water holding capacity (WHC)

Casein protein's water-holding capacity was determined by the method of Bhat et al. (2016). Casein (1g) was dissolved in 10 mL of DW and centrifuged for 30 min with agitation for a few seconds. The contents were centrifuged for 25 min at 3000×g after 30 min.

Finally, water holding capacity was determined using the below equation **(3.6):**

$$\text{Water holding capacity} = \frac{\text{Weight of the tube after the supernatant was released}}{\text{Weight of the tube with sample before water addition}} \times 100 \qquad (3.6)$$

3.2.11.3. Oil holding capacity (OHC)

Casein protein’s oil holding capacity was evaluated by Sarv et al. (2017). In pre-weighed centrifuge tubes, 0.5 g of native and modified casein protein was mixed with 6

mL of corn oil. For complete dispersion of the sample in oil, the tubes were agitated for one min. The samples were centrifuged at 3000×g for 25 min after 30 min of holding time. Before reweighing the tubes, the supernatant was pipetted and left inverted for 25 min for the oil to drain completely. Oil absorption was determined based on oil absorption per gram of casein protein as per the following equation **(3.7)**.

$$\text{Oil holding capacity} = \frac{\text{Weight of the tube after the supernatant was released}}{\text{Weight of the tube with sample before oil addition}} \times 100 \qquad (3.7)$$

3.2.11.4. Emulsification properties

For casein samples (native and treated), emulsifying properties were assessed following a modified version of the protocol described by Biswas and Sit (2020). The procedure involved homogenizing 1.5 g casein in 25 mL water at 2800×g for 30 s, followed by adding 12 mL sunflower oil and homogenizing again under the same conditions. The emulsion was split into two equal portions to measure emulsifying activity and stability. Emulsifying activity was determined by centrifuging one portion at 1100g for 5 min. The other portion underwent heating at 85°C for 15 min, cooling to room temperature, and centrifugation at 1100×g for 5 min to assess emulsifying stability. The emulsion activity was calculated based on the ratio between emulsion height and liquid layer height:

$$\textbf{Emulsifying Activity (\%)} = \frac{\text{Height of emulsified layer in the tube}}{\text{Height of total content of the tube}} \times 100 \qquad (3.8)$$

$$\textbf{Emulsification stability (\%)} = \frac{\text{Height of emulsified layer in the tube after heating}}{\text{Height of emulsified layer in the tube before heating}} \times 100 \qquad (3.9)$$

3.2.11.5. Bulk Density

The bulk density of casein (native and modified) was determined by the method of Butt and Rizwana, (2010). 10 g of native and treated casein were put into 100 mL graduated cylinder and was tapped several times on the laboratory bench till the isolates stopped settling and the values were expressed in g/cm^3.

3.2.11.6. Particle density

The particle density of the casein (native and modified) was determined by using the gas (helium) pycnometer (Gas Pycnometer PYC-100A). The sample was placed in the

sample cell and degassed by purging with a flow of dry gas (helium) by a series of pressurization cycles. The values were expressed in g/cm^3.

3.2.11.7. Color properties

Color attributes of the casein powder (native and modified) were determined by colorimeter (Ultrascan VIS, Hunterlab, USA) as per Biswas and Sit (2020) process. L*, a*, and b* values were noted. Values were represented by expressing parameters of L* (lightness), a* (redness), and b* (yellowness) respectively.

3.2.12. Properties of developed films

3.2.12.1. Film thickness and film solubility

Film thickness measurements followed the ASTM 065 method as described by Borah et al. (2017), using a micrometer to measure five random positions to the nearest 0.001 mm, with the average used for calculations.

Film solubility was determined according to Gontard et al. (1994), defined as the percentage of film dry matter solubilized in water at 25℃ over 24 h. The procedure involved conditioning film specimens in a silica gel desiccator until reaching constant weight. Film samples (2×2 cm) were weighed, immersed in 50 mL DW, and agitated at 125 rpm and 25°C for 24 h with periodic shaking. After removal from water, filtration was performed using pre-weighed filter paper, followed by drying at 105°C for 24 h until constant weight. Solubility was calculated using equation **(3.10)**.

$$S\ (\%) = 100\times \left[\frac{Wi-Wf}{Wi}\right] \qquad (3.10)$$

where S = solubility; w_i and w_f depict the initial and final weight of the films (dry weight basis) respectively.

3.2.12.2. Water vapor permeability

Water vapor permeability (WVP) assessment followed the E96-95 ASTM standard method (ASTM, 1995), utilizing a modified gravimetric cup technique (desiccant method) as described by Niu et al. (2021). The methodology involved securing film samples with rubber bands over circular permeation tube openings containing 8 mL DW (0% RH). The

film dimension (40 mm ×20 mm) was prepared to determine the water vapor transmission rate. These tubes were further put inside desiccators having saturated calcium chloride solution (75% RH) regulated around 25℃. In every film, 3 separate tubes were made taking measurements from numerous parts. After the attainment of steady state condition, the mass of tubes was reported every 24 h. The difference in RH facilitated water vapor transfer, resulting in mass differences.

WVP was calculated as follows:

$$\text{WVP} = \frac{\Delta m.x}{A.\Delta t \Delta p} \qquad (3.11)$$

Where: Δm/Δt represents the weight of moisture loss per unit time (g/h), A measures the area of film exposed to moisture transfer (m^2), x denotes thickness (mm), Δp shows water vapor pressure difference between adjacent sides of the film (kPa).

3.2.12.3. Film color

A Hunterlab colorimeter (Ultrascan VIS- USA) was employed to evaluate the color attributes of the PS, casein along with their blends using the protocol of Singh and Sit, (2023). The outcomes were articulated using the CIE Lab scale, established by the International Commission on Illumination. The measurements for L* (indicating lightness), a* (representing redness), and b* (depicting yellowness) were specifically noted and recorded. Color difference (ΔE) is determined by the below equation:

$$\Delta E = [(\Delta L^*)^2 + (\Delta a^*)^2 + (\Delta b^*)^2]^{1/2} \qquad (3.12)$$

Here, ΔL* stands for the disparity in brightness (Li*– L*), Δa* represents the variation in red-green chromaticity (ai*–a*), and Δb denotes the difference in yellow-blue chromaticity (bi* - b*). The "i" index signifies the reference value applied to each parameter.

3.2.12.4. Optical properties

The opacity of films was analyzed through the method described by Huntrakul et al. (2020) with some modifications. Film samples each into a rectangular shape were cut (20 mm × 40 mm) and inserted towards one edge of the cuvette. Individual absorbance of the film was determined by UV–Vis spectrophotometer (UV-2550, Shimadzu

International Trading Co., Ltd., Shanghai, China) with a blank cuvette taken as reference. Every analysis was performed in triplicates. The opacity in films was evaluated through the following equation:

$$\text{Opacity value} = \frac{A_{585}}{X} \quad (3.13)$$

A denotes absorbance measured at 585 nm while X denotes equivalent film thickness in mm, measured by micrometer. Low opacity value shows greater transparency in films.

Additionally, the light transmission of the films was assessed within the ultraviolet and visible range (200 to 800 nm) using a UV–Vis spectrophotometer (Agilent Cary 100, USA) following the methodology outlined by Huntrakul et al. (2020). Each film sample was cut into a rectangular piece (20 mm × 40 mm) and placed on one side of the cuvette. The absorbance of each film was measured using a UV-Vis spectrophotometer (Agilent Cary 100, USA), with a blank cuvette serving as the reference.

3.2.12.5. Mechanical properties

The mechanical properties (tensile strength and elongation at break percentage) were evaluated using a Texture Analyzer (TA-XT, Stable Micro Systems, UK) following the ASTM D-882-91 method (1996), utilizing an AMTG probe with six sample measurements averaged. The initial parameters were set to 30 mm separation distance and 10 mm/s speed. Film specimens were cut into strips measuring 20 mm × 40 mm and conditioned for 48 hours. Thickness measurements were taken at 5 points on each strip prior to testing. Under tension mode, the strips were extended at 0.8 mm/s until breakage, with force and distance recorded throughout. The testing configuration included a 5 kg load cell with speeds of 2 mm/s (pre-test), 3 mm/s (test), and 10 mm/s (post-test), a 75 mm distance setting, and a 10 g trigger force. Tensile strength (TS) was calculated by dividing the maximum force (FM) by the film cross-sectional area (A).

Both tensile strength (TS) and elongation percentage (E) at break were determined using the specified equations:

$$\text{TS} = \frac{Fm}{A} \quad (3.14)$$

TS denotes tensile strength in (MPa); Fm represents maximum force (N) and A is the cross-sectional area of film (thickness x width in m^2);

$$E = \frac{d_r}{d_0} \times 100 \qquad (3.15)$$

E gives the elongation (%); d_0 shows the distance onset of separation (cm); and d_r denotes the distance of rupture (cm).

3.2.12.6. Sealing properties

Developed films (PS, casein, and blended) were sealed utilizing an impulse heat seal tester (TP-701-B; Tester Sangyo Co., Ltd.) following the process described by Das and Choudhury (2016). Two film sections (5 cm × 2 cm) were heat-sealed by positioning one atop the other and applying foot pedal pressure (0.2 MPa) at temperatures near their melting points for durations ranging from 0.2 to 2.0 sec. These sealed film strips were left to dry at 23℃ for 16 h. The sealing strength of the film was assessed using a Texture Analyzer (TA-XT, Stable Micro Systems, UK) until detachment occurred from the sealed area. The maximum force per unit width of the film needed to strip off the sealing portion was recorded. Seal strength was determined using Equation **(3.16)**. Additionally, the sealing efficiency of the blended films was calculated to evaluate the quality of the seal in terms of strength and integrity using Equation **(3.17)**.

$$\text{Seal strength } \left(\frac{\text{N}}{\text{m}}\right) = \frac{\text{Peak force}}{\text{Film width}} \qquad (3.16)$$

$$\text{Seal efficiency } (\%) = \frac{\text{Peak force}}{\text{Tensile force}} \times 100 \qquad (3.17)$$

Where tensile force is the force (N) obtained from tensile strength testing of single film and peak force (N) is the maximum force obtained from seal testing.

3.2.12.7. Thermal properties

Thermal degradation characteristics in developed PS and casein-based films were measured by use of (TGA) a Shimadzu TGA-50 thermo-gravimetric analyzer following the More et al. (2022) procedure. All developed films were scanned under 30 to 600℃ at a heating rate of 10℃/min under high-pure N_2 atmospheric conditions. A standard aluminum pan was placed containing about 10-12 mg of each film sample with an empty

pan serving as a reference.

3.2.12.8. Biodegradation of starch-based films

To check biodegradability, a soil burial test was performed over 45 days, simulating aerobic composting by ISO 14855-1:13, with modifications as detailed by La Fuente et al. (2023). The degree of decomposition was observed through visual inspection and mass changes. The developed film's size (40mm × 20mm) was buried inside soil around 20 cm deep from the surface. Subsequently, the soil environment is regulated at 7±1pH with 32±2°C. Soil moisture was kept around 5-10%. Films were scaled down and placed inside enrichment soil. For two weeks, samples were monitored every 48 h. The frequency of observations was cut to once a week after the third week. The observations were based on the reduction of the film's area and were finalized when the samples were completely degraded by the loss of their area. Daily, 10 mL of water was poured into the soil, and the ultimate weights were examined after 15–30 days. The samples were taken out after a specific duration, cleaned with ethanol and water, and then dried at 50°C to a constant weight. The sample's weights were measured before and after drying. The % weight loss in samples was determined as follows:

$$\text{Weight loss} = \left[\left[\frac{(M_0 - M_1)}{M_0}\right] \times 100 \right. \qquad (3.18)$$

M_O depicts the weight of the original films before the test and M_1 denotes the weight of residual films after drying until constant weight is gained.

3.3. Statistical Analysis

The experimental results, presented as mean values with their corresponding standard deviations, were acquired through SPSS statistical software (version 26, SAS Institute Inc., Cary, NC, USA). Statistical distinctions were evaluated using a one-way analysis of variance (ANOVA) followed by Duncan's multiple range test (DMRT), where significance was established at a threshold of $(p<0.05)$.

3.4. Results and discussions

3.3.1. Properties of PS

3.3.1.1. Swelling power and solubility of native and modified starches

Swelling power and solubility are crucial for determining the functional properties of starches, significantly impacting their applications in the food industry and beyond. Understanding these properties allows for better utilization and innovation in starch-based products and is also vital for the development of effective starch-based films. Swelling power reflects the ability of starch to retain water at certain temperatures. Solubility measures the quantity of amylose that leaches out from starch granules due to diffusion and dissociation during the swelling process (Li et al., 2019). Significant differences *($p<0.05$)* in the swelling power and solubility have been reported between the modified and native PS. The swelling power ranged from 21.2 to 30.9 g/g and the solubilities ranged from 10.5 to 17.6%. The values are presented in **Table 3.2**. Enhanced solubility (17.6%) is observed in the case of native PS (NPS) which can be attributed to the de-polymerization and deterioration of the starch granular structure. The granular pattern of the starch allows water to permeate the amorphous portion of the granule during heating, causing hydration and little swelling losing the ability to act as a structural reinforcement (Subroto et al., 2019). Heat moisture-treated (HMT) starches showed a considerably lower solubility (10.5%) than annealed (ANN) (14.04%) and native starches (17.6%) indicating that the molecules of amylose and amylopectin interact more strongly, which prevents them from leaching out of the granules (Gomes et al., 2005). As compared with ANN and native starch, HMT causes a greater reduction in swelling power due to the rearrangement of starch granules within the starch matrix (Brahma and Sit, 2020), which facilitates further interaction between the starch functional groups, resulting in the formation of double-helical clusters of amylopectin side chains. The increased crystallinity of starch is explained by this (Araujo-Farro et al., 2010; Zavareze et al., 2012). Swelling of starch granules by HMT decreased through molecular rearrangement of granules, formation of amylose-lipid complexes, degradation of amylopectin molecules, increased interaction between amylose chains, and changes in interactions between amorphous and crystalline matrixes (Singh et al., 2009; Marboh and Mahanta, 2021) Thus, the lower solubility and swelling power of the modified PSes may

indicate differences in the structure, molecular weight, or phosphorous content, which could affect the properties of films made from these starches.

Table 3.2 Solubility, swelling power, and color properties of native, annealed, and heat-moisture-treated PS

Starch sample	Solubility (%)	Swelling Power (g/g)	Color Parameters			
			L*	a*	b*	DW
NPS	17.6±1.98^{a}	30.9±2.25^{a}	42.98±0.45^{c}	0.18±0.11^{c}	2.02±1.50^{b}	35±1.89^{b}
ANNS	14.04±0.79^{b}	25.7±1.79^{b}	46.33±0.74^{b}	0.25±0.23^{b}	3.40±1.21^{a}	38.75±0.96^{a}
HMTS	10.5±0.51^{c}	21.2±1.24^{c}	47.07±0.67^{a}	0.66±0.75^{a}	3.39±0.74^{a}	39.04±2.33^{a}

Values are reported as mean ± standard deviation of three replications. Means followed by the same superscript small letters within a column are not significantly different *(p>0.05).* NPS- Native potato starch, HMTS- Heat-moisture treated starch, ANNS- Annealed starch

3.3.1.2. Color properties of native and modified starches

The color parameters (L*, a*, and b*) of starch pastes exhibited the following ranges: L* (lightness) ranged between 42.98 and 47.07, a* (redness) between 0.18 and 0.66, and b* (yellowness) between 2.02 and 3.40, as shown in Table 3.2. The degree of whiteness (DW) was calculated for each sample. Statistical analysis revealed significant differences between native and modified starches, with heat-moisture treated (HMT) and annealed (ANN) starches showing significantly higher L*, a*, and b* values ($p < 0.05$) compared to native samples. While native starches displayed lower L* values, modified starches demonstrated higher lightness values (L* and DW). According to Sit and Deka (2013), starches exhibiting higher L* values combined with lower a* and b* values are suitable for applications requiring visual clarity and consistency. The lowest a* values were observed in native and ANN-treated starches, while HMTS showed the highest values. Native potato starch (NPS) exhibited lower b* values compared to modified variants. These color parameters aligned with those reported by Araujo-Farro et al. (2010) for quinoa starch. All samples showed color coordinates between yellow and red, with a stronger tendency toward yellow. DW values ranged from 35 to 38.04, with modified HMT displaying the highest values, indicating superior whiteness and purity. As noted by Biswas and Sit (2020), the minimal color changes in ANNS likely resulted from gentle

treatment and washing processes, while the more pronounced color alterations in HMTS were attributed to higher processing temperatures.

3.3.1.3. Freeze-thaw stability of native and modified starches

Regarding freeze-thaw stability, syneresis percentage serves as an indicator of product quality deterioration, with lower values after frozen storage indicating superior stability. **Table 3.3** presents the syneresis values over five freeze-thaw cycles, showing progressive increases with storage time. Significant variations (*p>0.05*) were observed between modified and native PS pastes across the cycles. Native starch exhibited greater syneresis increase (15.90% to 24.04%) compared to modified variants. Hoover (2010) attributed water exudation from starch gels to enhanced intermolecular and intramolecular hydrogen bonding among starch chains (amylose-amylose, amylose-amylopectin, and amylopectin-amylopectin) during frozen storage. Both HMT and ANN modifications reduced gel water loss compared to native starches. HMTS demonstrated superior freeze-thaw stability with lower syneresis (14.60% to 20.97%) compared to ANNS (12.91% to 22.85%) and native starch. Brahma and Sit (2020) explained that during HMT, water molecules become bound within the amylose-amylopectin crystalline structure, making their escape from the gel matrix more difficult. Similar reductions in syneresis percentage following heat-moisture treatment were reported by Singh et al. (2009) and Deka and Sit (2016) in their studies of Indian water chestnut and taro starches, respectively.

Table 3.3 Percent syneresis of native, annealed and heat-moisture treated PSes up to five freeze-thaw cycles

Starch sample	Cycle 1	Cycle 2	Cycle 3	Cycle 4	Cycle 5
NPS	15.90 ± 0.84^{aC}	17.98 ± 1.57^{aB}	20.78 ± 1.21^{aB}	23.03 ± 0.80^{aB}	24.04 ± 0.70^{aA}
ANNS	12.91 ± 0.66^{bC}	16.25 ± 0.32^{bBC}	18.18 ± 0.46^{bB}	19.17 ± 1.02^{bB}	22.85 ± 0.88^{bA}
HMTS	14.62 ± 1.26^{abD}	15.02 ± 0.48^{bC}	16.21 ± 0.64^{cBC}	18.16 ± 1.10^{bB}	20.97 ± 1.35^{cA}

Values are reported as mean ± standard deviation of three replications. The means followed by the same capital letter superscripts within a row for the same parameter, and the means followed by small letter superscripts within a column are not significantly different *(p>0.05).* NPS- Native potato starch, HMTS- Heat-moisture treated starch, ANNS- Annealed starch

3.3.1.4. Rheological properties of native and modified starches

The rheological characteristics of products help determine their quality and sensory attributes under shear forces. Starch pastes demonstrate visco-elastic properties, with their dynamic and steady-state rheological parameters presented in **Table 3.4** and viscosity-shear rate relationship shown in **Fig. 3.1.** The Ostwald de Waele model provided excellent fit to the data ($R^2 > 0.99$ for all starches). Both native and modified PS exhibited pseudoplastic (shear-thinning) behavior, consistent with findings by Singh and Kaur (2017) for oat starches and Devi and Sit (2019) for barley starch. The consistency index 'K' and flow behavior index 'n' showed significant decreases in ANNS and HMTS. These modified starches demonstrated enhanced pseudo-plasticity, with values approaching '0' compared to 0.1625 for native starch. Celik et al. (2018) attributed this non-Newtonian fluid behavior to molecular displacement under high shear forces. The lower 'n' values in ANN and HMT starches indicated weakening intermolecular bonds with increasing shear. The elastic properties are represented by storage modulus (G′), while loss modulus (G″) measures dissolution energy associated with viscous motions. Significant variations ($p<0.05$) were observed in G', G", η*, and phase shift angle (δ) across samples. Storage modulus values exceeded loss modulus, indicating strong elastic characteristics in modified starches. G' increased with temperature due to expanded starch granules occupying more solution volume and increasing stiffness. According to Trung et al. (2017), G" increases resulted from amylose leaching from swollen granules forming continuous networks with viscous behavior. Similar patterns were reported by Marboh and Mahanta (2021) in sohphlang (*Flemingia vestita*) tuber starch after HMT and annealing modifications. Hu et al. (2020) suggested that increased G' and G" values might result from reduced swelling power and solubility. Complex viscosity (η*), measuring overall flow resistance, decreased with increasing frequency, demonstrating shear-thinning behavior across all starches. The phase shift angle (δ), ranging from 8.46° to 21.53°, indicates the stress-strain state difference between ideal solid (0°) and ideal liquid (90°). Modified PS pastes showed significantly lower dynamic moduli (G' and G") and η* values compared to native samples, attributed to altered granular integrity from increased water uptake. Xu et al. (2018) noted that structural, size, and compositional changes affected granular viscosity behavior. G' values consistently exceeded G" across all frequencies, indicating predominant elasticity in PS starches. As noted by Kaur et al. (2012), G' should be frequency-independent and significantly higher than G" (G'≫G"). The study demonstrated

that hydrothermal treatment could enhance visco-elastic modulus in NPS, with modifications significantly altering starch flow behavior, supporting their application in film production

Table 3.4 Dynamic and steady state rheological properties of native, annealed and heat-moisture treated PS

Starch Sample	Dynamic Rheology				Steady State Rheology		
	Storage Modulus (G') (Pa)	Loss Modulus (G'') (Pa)	Complex Viscosity (η*) (Pa. s)	Phase angle (δ) (°)	K (Pa.s^n)	N	R^2
NPS	20549.63±202.56^a	3061.25±236.15^a	505.67±35.10^a	8.46± 0.95^c	228.12±5.63^a	0.1625±0.011^a	0.9912±0.04^a
ANNS	813.69±50.51^b	320.94±28.35^b	21.25±2.96^b	21.53± 1.64^a	125.95±2.54^b	0.0300±0.002^b	0.9982±0.03^a
HMTS	704.27±13.57^c	219.95±17.55^c	17.92±1.87^c	17.34± 1.54^b	114.18±2.39^b	0.0298±0.001^b	0.9992±0.03^a

Values are reported as mean ± standard deviation of three replications. Means followed by the same superscript small letters within a column are not significantly different (p>0.05). NPS- Native potato starch, HMTS- Heat-moisture treated starch, ANNS- Annealed starch

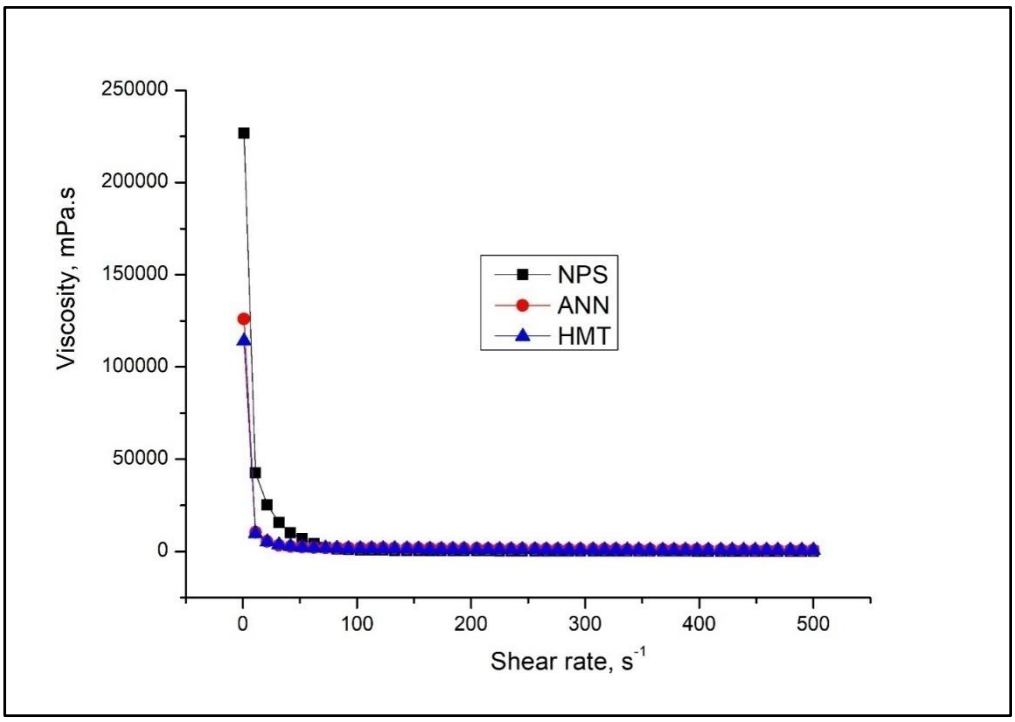

Fig. 3.1 Change in viscosity of native and modified starch pastes with shear rate (NPS- native potato starch, ANN- Annealed starch, HMT- Heat-moisture treated starch

3.3.1.5. Pasting properties of native and modified starches

The pasting characteristics of native and modified PS are shown in **Table 3.5.** According to Whistler et al. (2012), pasting property measurements enable identification of amylograph response changes due to material or process variations, estimation of starch processing behavior, and determination of initial processing equipment parameters. PS demonstrated unusually high peak viscosity, which Liu et al. (2016) attributed to phosphate groups present in the amylopectin region. Trung et al. (2017) noted that HMT significantly altered starch pasting profiles through chain linkages in granule amorphous regions, while ANN treatment effects varied by starch type. Peak viscosity measurements ranged from 6679 cP to 9621 cP. HMT modification resulted in increased pasting temperature (PT) while decreasing peak viscosity (PV), breakdown viscosity (BD), and setback viscosity (SB). Modified starches showed reduced PV values: HMT at 8156 cP and ANN at 6679 cP. The PV reduction in both modifications correlated with moisture content and decreased swelling power. Subroto et al. (2019) suggested that increased inter and intra-molecular hydrogen bonding in starch chains and amylose breakdown in HMT starches contributed to the PV decrease (8156 cP). Pasting temperature, marking the onset of paste thickening, typically increases with HMT. Deng et al. (2023) observed that

shortened chains in HMT-modified starches led to reduced chain entanglement during pasting, indicating strengthened PS granules. The elevated pasting temperature in annealed starch, as noted by Xu et al. (2018) and Hu et al. (2020), indicated increased gelatinization temperature requirements due to stronger granule linkages developed during treatment, resulting in greater swelling resistance. Final viscosity (FV) was lower in annealed starches (7203 cP) compared to HMT variants (7575 cP). This aligns with Cai & Shi's (2010) findings of reduced FV in annealed long-grain and waxy rice starches. Breakdown viscosity, indicating granule firmness under sustained agitation and heat, showed significant reduction in both HMTS (2497 cP) and annealing (41 cP). The BD decrease correlated with reduced granule swelling and amylose degradation during HMT. HMTS demonstrated lower setback viscosity compared to both native and ANNS-treated starch. Less SB depicts that modified starches possessed a lower potential to retrograde in comparison with native starches that depend upon factors like the leaching of amylose, its chain length, and granular structure (Shi et al., 2013). The findings were similar to HMT-treated canna starches (Watcharatewinkul et al., 2006). Jacobs and Delcour (1998) analyzed that annealing increased the hold and final viscosities in the case of wheat, rice, and pea starches compared to NPS. Literature reports proposed that annealing effects on starch pasting behaviors severely vary on structural attributes and the analysis criterion. Results were in agreement with the findings of Hormdok and Noomhorm (2006) where a reduction in the viscosity parameters of HMT rice starch was obtained. A decrease in BD indicated that hydrothermally modified starch granules were consistent with continuous heating and shearing conditions that resist degradation when compared with other studies. The same trend was observed for cereal starches (Wang et al., 2021) along with maize starch (Zou et al., 2020). The pasting behavior thus obtained after hydrothermal modification could help enhance starch processing with improvement in the pasting properties of PS. Suggesting the presence of strong bonding forces within the granular interior. The HMT may make the granules resistant to deformation by strengthening the intragranular binding force, and it was speculated that in the annealed starch, swollen gelatinized granules were more rigid, contributing significantly to high cold-pasted viscosity (Singh et al., 2005).

Table 3.5. Pasting properties of native, annealed, and heat-moisture-treated PS

Starch sample	Pasting Temperature, PT (°C)	Peak Viscosity, PV (cP)	Hold Viscosity, HV (cP)	Final Viscosity, FV (cP)	Breakdown Viscosity BD (cP)	Setback Viscosity, SB (cP)
NPS	70.3±0.12^{c}	9621±130^{a}	3244±103^{c}	3759±92^{b}	6377±282^{a}	515±18^{a}
ANNS	77.6 ±1.98^{b}	6679 ±75^{c}	6638±128^{a}	7203±124^{a}	41±03^{c}	524±25^{a}
HMTS	86.7 ±1.35^{a}	8156 ±30^{b}	5659±212^{b}	7575±385^{a}	2497±89^{b}	508±38^{a}

Values are reported as mean ± standard deviation of three replications. Means followed by the same superscript small letters within a column are not significantly different (p>0.05). NPS- Native potato starch, HMTS- Heat-moisture treated starch, ANNS- Annealed starch

3.3.2. Properties of casein

3.3.2.1. Protein solubility

It is essential to understand protein solubility for understanding protein hydration which is a reliable indication of the properties of protein aggregation and conformational changes, but also an indicator of how protein foams, emulsifies, gels, produces films, and is viscous when emulsified (Jambrak et al., 2008). Protein solubility differed significantly ($p<0.05$) between treated and native casein samples and is presented in **Table 3.6**. Protein solubility increased with the native and treated ones. After ultrasonication, the protein solubility was discovered to be increased, and it was greatest when the treatment time was 30 min (76.43 %), followed by the treatment for 15 min (73.43 %). The hydrophilic amino acid residues are directed toward the water in high-intensity ultrasound by altering their shape and structure, which increases protein solubility (Biswas and Sit, 2020). Autoclave-treated samples showed protein solubility values lower than ultrasound-treated ones; AC 30 (69%), and AC 15 (67.04 %) but higher than native casein (63.6 %). With increased treatment effectiveness or duration, the solubility of the protein increased significantly. Using ultrasound may disrupt weaker bonds, such as H-bonds, in the protein thus altering its conformation and increasing its solubility (Jambrak et al., 2008). Several researchers have noticed an enhancement in temperature with treatment that helps to enhance solubility (Jambrak et al., 2009; Jiang et al., 2014), which showed that ultrasound treatment's ability to increase protein solubility. Autoclave treatment significantly

improved the solubility of casein particles, especially at longer processing times (Ogechukwu and Ikechukwu, 2017). Wang and Johnson (2001) demonstrated enhanced emulsifying, foaming, and solubility characteristics of soybean protein concentrate after autoclave treatment along with Rico et al. (2020) for wheat bran and soy protein concentrate (Moon, 2002).

Table 3.6: Functional properties of native and treated casein

Sample	Protein Solubility (%)	Emulsification Activity (%)	Emulsification stability (%)	Water holding capacity (%)	Oil holding capacity (%)	Bulk Density (g/cm^3)	Particle density (gm/cm^3)
NC	63.6 ± 1.98^{e}	53.13 ± 0.57^{e}	43.33 ± 0.18^{d}	113.99 ± 0.98^{d}	105.41 ± 0.93^{e}	0.695 ± 0.003^{c}	1.348 ± 0.006^{a}
ATC 15	67.04 ± 0.79^{d}	53.33 ± 0.57^{d}	46.66 ± 0.66^{c}	116.26 ± 0.76^{c}	106.64 ± 0.83^{d}	0.730 ± 0.003^{a}	1.345 ± 0.06^{b}
ATC 30	69 ± 0.51^{c}	56.40 ± 0.47^{c}	49.66 ± 0.47^{b}	117.57 ± 0.58^{b}	107.05 ± 1.02^{c}	0.709 ± 0.002^{b}	1.329 ± 0.003^{c}
UTC 15	73.43 ± 0.56^{b}	57.1440 ± 0.22^{b}	52.30 ± 0.61^{a}	117.38 ± 0.89^{b}	107.96 ± 1.01^{b}	0.66 ± 0.001^{d}	1.327 ± 0.001^{c}
UTC 30	76.43 ± 0.76^{a}	57.84 ± 0.32^{a}	52.42 ± 0.42^{a}	120.515 ± 1.02^{a}	108.43 ± 1.23^{a}	0.62 ± 0.002^{e}	1.324 ± 0.008^{d}

NC- Native Casein, UTC- ultrasound treated casein, ATC- Autoclave treated casein. Values are reported as mean ± standard deviation of three replications. Means followed by the same superscript small letters within a column are not significantly different ($p>0.05$).

3.3.2.2. Influence of modification on the particle density

The untreated and treated casein's particle densities are presented in **Table 3.6**. The particle density of the native and modified samples varied effectively with treatment exposure of ultrasound and autoclave. Native casein samples showed a particle density of 1.348 gm/cm^3. ATC 30 showed 1.329 gm/cm^3 and ATC 15 showed 1.345 gm/cm^3. UTC 30 showed 1.324 gm/cm^3 while UTC 15 showed 1.327 gm/cm^3 values of particle density respectively. Ultrasound waves can reduce particle size (Shen et al., 2017). Upon ultrasonic modification, the particle density may decrease due to an unfolded or rearrangement of the protein's structure (Flores-Jiménez et al., 2019). According to Yanjun et al., (2014) findings, ultrasonic modification decreases the particle size of milk protein concentrate respectively. A significant reduction in particle size *($p<0.05$)* was reported when whey protein concentrate was modified using ultrasonic baths of 40 kHz for 15- and 30-min duration (Jambrak et al., 2014). Autoclave treatment significantly ($p<0.05$)

diminished the particle size with an exposure time of 15 and 30 min. In response to heat treatments, hydrophobic amino acids buried within native proteins were exposed, causing a rapid decline in particle breakdown, and droplet size reduction is facilitated by an increase in interfacial tension. Smaller particle sizes are advantageous factors in film formation (Li et al., 2020). When compared to other treatment techniques, ultrasonication is successful at both reducing the size of the biopolymer particle and promoting the dispersion within the matrix enhancing its packaging efficiency (Shen et al., 2017).

3.3.2.3.Influence of modification on water holding capacity (WHC)

Water holding is likely the most significant characteristic of protein in foods, as casein proteins form a stable dispersion and improve other properties such as foaming, gelling, and emulsifying and are closely related to solubility. **Table 3.6** represents the water holding capacity (WHC) of untreated including treated casein. UTC 30 showed the highest water-holding capacity upon treatment at (120.51%) followed by UTC 15 (117.38 %). Additionally, ATC 30 showed water solubility (117.57 %) and ATC 15 showed (116.26 %) higher than native casein samples (113.99%). The current study demonstrates that the WHC increased from 113.99% in the untreated sample up to 120.51% for a treatment duration of 30 min. A further increase in the WHC was seen if the treatment's duration or intensity was increased. There is a possibility that the enhancement in WHC for casein with ultrasound treatment might be attributed to the unfolding of polypeptide chains that exposed the hydrophilic clusters (Mi et al., 2021). Autoclave treatment may displace larger particles or any previously gathered proteins because of steam and pressure treatments. Additionally, it might stop big aggregates from forming through high-shear mixing while cooking (Li et al., 2020).

3.3.2.4. Influence of modification on oil holding capacity (OHC)

Table 3.6 presents the results of the oil holding capacity (OHC) of native and treated casein. In the present study, the oil holding capacity (OHC) of the ultrasonically treated samples was significantly greater ($p<0.05$) compared to native casein. The native casein showed a value of 105.41%. The ultrasound-treated sample showed a value of UTC 30 (108.43%) and UTC 15 (107.96%). Autoclave-treated samples showed values of 107.05% for 30 min and 106.64% for 15 min. It has been suggested that the increase in OHC of casein is caused by the collapse of cavitation bubbles around the protein

molecules, as well as the conformational changes in the protein's structure brought on by the ultrasonication of the polypeptide chains. Different degrees of the unfolding of polypeptide chains may explain differences in OHC between the ultrasonically treated samples, depending upon both the intensity of ultrasonication and the duration of treatment (Kresic et al., 2008). Autoclave treatment showed a considerable impact on the ability of oil absorption in casein samples. However, when modified hydrothermally, isolates had much better oil absorption capabilities (Seifdavati and Taghizadeh, 2012).

3.3.2.5. Influence of modification on emulsifying properties

Mostly, proteins are used in food products as emulsifying agents in frozen desserts, salad dressings, including minced meat, etc., and they are also capable of forming viscoelastic films at oil-water interfaces. In oil/water systems, proteins can create a homogenous emulsion by combining two immiscible liquids (Han et al., 2020). The (emulsifying activity) EA and (emulsifying stability) ES of the untreated and treated casein proteins are presented in **Table 3.6** presenting significant differences ($p<0.05$) among the caseins. Ultrasonication-treated casein exhibited the maximum stability and emulsifying ability, respectively (57.84 %) and (52.42 %). Ultrasonication improved stability and emulsifying activity were both more apparent when the treatment duration or intensity was longer. Enhancing the emulsifying ability of proteins by ultrasound has a significant impact (Mi et al., 2021). A protein's emulsifying property can be related to molecular flexibility, surface hydrophobicity, surface charge, and protein solubility (Arzeni et al., 2012; De Maria et al., 2016). Autoclave-treated for 30 min showed 56.40% emulsification activity and 49.66% emulsification stability higher than the native ones. NC (40.00%) showed the lowest emulsifying stability and activity (43.33%) and (53.13%). Hydrothermal treatment can reduce protein droplet size, resulting in an emulsion with a narrower size distribution and smaller droplets than crude protein (Qamar et al., 2019). Increasing the hydrothermal treatment time improved the emulsifying capacity. Overall, UTC 30 had the highest emulsifying capacities among the five samples. Hydrothermal modification exposed hydrophobic units, which made it easier for them to interact with the nonpolar solvent, improving surface activity and emulsion qualities (De Maria et al., 2016). The EA and ES in this study are quite comparable to those previously reported by Khan et al. (2011) for heat treatment provided to extract rice bran protein isolates. Proteins receive sufficient energy from heat and their hydrophobic groups are exposed related to

the separation of protein subunits and disruption of hydrophobic interactions (Aryee et al., 2018). The application of ultrasounds also enhances the emulsifying abilities of whey proteins, leading to a better dispersion of lipids inside the films (Meng et al., 2021). The decrease of particle size by ultrasound raises the protein molecular flexibility and extension around the oil droplets leading to improved adsorption at the oil-water interface and the production of denser films and thicker layers (Li et al., 2021). Galus and Kadzinska, (2015) utilized the emulsifying properties of casein to improve the moisture-barrier qualities of casein-lipid emulsion films. When those emulsion films were formed, lipids improved water resistance, whereas casein increased structural cohesion, linked the film to wet surfaces, and lessened the waxy look (Wittaya, 2012).

3.3.2.6. Influence of modification on the bulk density

Particle size, interparticle tensions, and the TS of contact points all have an impact on bulk density, which characterizes the behavior of materials during packaging. An increase in bulk density indicates economical packaging, but it has the drawback of being unsuitable for infant foods (Khan et al., 2011). Bulk density values varied significantly ($p<0.05$) from 0.62 g/cm^3 to 0.730 g/cm^3 which are presented in **Table 3.6**. Casein got firmer with extended treatments. Particle size changes were likely the cause of changes in bulk densities. Changes in bulk densities were probably the result of changes in particle size (Mi et al., 2021). Ultrasound modification significantly decreased ($p<0.05$) the bulk density of the protein isolates concerning the autoclave treatment, possibly due to the ultrasound causing larger structures. The effect of autoclaving on bulk density might be linked to its effect on the particle size which enhanced from 0.709 g/cm^3 to 0.730 g/cm^3 with the increase in the duration time.

3.3.2.7. Color properties of native and modified casein

Color has an important effect on the state of packaging films as it influences the product packaging appearance. Determinants of color L*, a*, and b* of the native and modified casein are represented in **Table 3.7**. Results exhibited to L* (lightness) ranged from 66.075 to 81.767, a* (redness) showed from -0.17 to 0.59, and b* (yellowness) varied from 9.235 to 29.35 values. Under the ideal circumstances for ultrasonic processing, excellent color qualities may be produced. The a* value decreased after 30 min of ultrasonic treatment, although the L* value significantly increased. Zhang et al. (2019)

found that the nanocomposites L* value made with PVA concentrations improved when coupled with graphene oxide (GO) and zinc oxide nanoparticles (ZnO NPs) marginally when applied with ultrasonic treatment for 30 min, however, a* and b* values dropped subsequently. It seems that as a result of the film-forming components' homogeneous dispersion, ultrasonic treatment is advantageous for increasing film lightness (Mi et al., 2021). The uniform distribution within the additives inside the polymeric matrix, and disruption of the particles caused by ultrasound including reduction of the typical droplet size of the additives are the main causes of the color shift in films generated by ultrasound modification (Jambrak et al., 2009). Autoclave treatment led to a recognizable color change in casein. As treatment time progressed, all samples got a little bit darker because Maillard reaction products were produced, although the darkening extent was not significant. The extent of redness (a* values) increased with increasing treatment time i.e., the color varied towards red from green. The production of dark-colored Maillard reaction products is likely what caused the transition from green to red. Yellowness (b* values) of samples also increased with the treatment time. As treatment time increased, there was generally a gradual enhancement in yellowness. This was probably brought on through the breakdown of natural yellow pigments and the production of chemicals from the Maillard reaction. Additionally, as compared to Galus and Kadzinska (2016) and Osés et al. (2016), a* values for films treated with heat were lower whereas b* values were greater.

Table 3.7 Color properties of native and treated casein

Casein	L*	a*	b*
NC	75.045 ± 0.45^{c}	0.59 ± 0.11^{c}	17.68 ± 1.50^{b}
ATC 15	66.075 ± 0.74^{e}	3.81 ± 0.23^{a}	29.35 ± 1.21^{a}
ATC 30	71.941 ± 0.67^{d}	2.21 ± 0.75^{b}	22.825 ± 0.74^{a}
UTC 15	80.856 ± 0.45^{b}	-0.17 ± 0.002^{e}	9.97 ± 0.012^{d}
UTC 30	81.767 ± 0.45^{a}	-0.2 ± 0.006^{d}	9.235 ± 0.021^{e}

Values are reported as mean ± standard deviation of three replications. Means followed by the same superscript small letters within a column are not significantly different ($p>0.05$). NC- Native Casein, UTC- ultrasound treated casein, ATC- Autoclave treated casein

3.3.3. Properties of film

3.3.3.1. Thickness

The thickness of a food packaging film plays a crucial role in determining its key properties. Specifically, it significantly affects the film's water vapor permeability (WVP), opacity, and tensile strength (TS) (Mihilca et al., 2021). There was no statistically significant variation between the films *(p>0.05)* obtained from PS and casein as displayed in **Tables 3.8 and 3.9**. However, the thicknesses of the PS and casein blended films displayed significant variations *(p<0.05)* across different proportions of film-forming components, as detailed in **Table 3.10**. **Fig. 3.2 and 3.3** showcase the appearance of PS and casein blended films, highlighting differences when prepared from pure PS and casein too. Additionally, **Fig. 3.2** presents the appearance of various starch and protein-concentrated blended films from (10:90, 20:80, 30:70, 40:60, 50:50, 60:40, 70:30, 80:20, 90:10). It's worth noting that films were prepared with concentrations of 10:90, 20:80, 80:20, and 90:10 starch and protein but were excluded from further study due to brittleness. Film microstructure and thickness affect largely on optical parameters too, which are strongly influenced by the matrix's internal and surface heterogeneity (Zavereze et al., 2012). The film thicknesses of the PS (native and modified) varied from 0.12 to 0.15 mm **(Table 3.8)**. Starch films (PS) prepared from HMT (HMTF) produced smoother and softer films having 0.13 mm thicknesses **(Table. 3.8)**. Annealed (ANNF) obtained thinner and firmer films with a thickness (of 0.12mm). Due to the thicker generation of gelatinized starch in native counterparts, native PS films (NPSF) were the thickest (0.15 mm). The thickness values of the PS films obtained were similar to those observed by Wawro et al. (2019), who revealed the thicknesses in PS varied between 0.063 and 0.140 mm. The result is in agreement with Zhang et al. (2018) who reported near thicknesses in nano-SiO_2 films of varied sizes. The thicknesses of the casein films (native and modified) ranged from 0.27 to 0.318 mm **(Table 3.9)**. The biopolymeric films did not vary statistically significantly *(p>0.05)* from one another, though casein-based films prepared were smoother and soft and were visually observed as transparent and yellow. As the film samples in this study were made from identical raw materials and contained the same amount of plasticizer, no noticeable changes between the samples were found. There was no noticeable change in the film's thickness when *L. rhamnosus* GG cells were incorporated into probiotic-contained edible films (Lee et al., 2020). The thickness of the film is greatly regulated by the ingredients, the amount and kind of plasticizers employed along with film

formation procedure. For the PS and casein blended films observations ranged between 0.34 mm to 0.49 mm in film thickness, a crucial factor for optimal functionality impacting structural consistency, particularly in their role as thin conducting films **(Table 3.10)**. Films crafted solely from native PS and casein measured the thinnest at 0.13 mm and 0.302 mm, respectively (Dutta and Sit, 2022). However, films combining starch and protein exhibited increased thickness compared to single-ingredient films, aligning with findings from composite edible films like wheat starch and whey-protein isolate (Basiak et al., 2015). The 50:50 proportionate blended films (50% starch and 50% protein) seemed to offer optimal functionality, showcasing a thickness of 0.42 mm, striking a balance between pure starch and protein films in a 1:1 ratio. Similarly, films with 25% starch and 25% protein isolate fell between the thickness values of 1:1 ratio films and pure protein isolate films (Huntrakul et al., 2020). Notably, films with higher starch proportions (70% starch and 30% protein, and 60% starch and 40% protein) measured 0.49 mm and 0.46 mm, respectively, surpassing the thickness of films made purely from these components. This increase suggests that adding starch contributed to a thicker film matrix, supported by prior studies on PS and other plasticizer ratios (Fonseca et al., 2018). The trend indicates that higher starch proportions led to thicker films compared to higher proportions of protein, potentially due to starch reinforcing hydrogen bonds and augmenting film thickness. Similar results showing increased film thickness with starch concentration (3%–5%) have been reported for sorghum starch films (Biduski et al., 2017). However, it's interesting to note that the blended film thickness at a 50:50 starch: casein ratio was lower compared to other starch-casein proportions (60:40 and 70:30). The addition of protein concentrate resulted in a comparatively lower thickness of the composite biodegradable film (Sukhija et al., 2016). Similar decreases in the thickness of pea starch film upon adding peanut protein isolate and composite biodegradable film from whey protein concentrate and psyllium husk have been previously reported (Sun et al., 2013; Sukhija et al., 2016).

Fig. 3.2: Appearance of 1) Potato starch (PS) film 2) Casein film

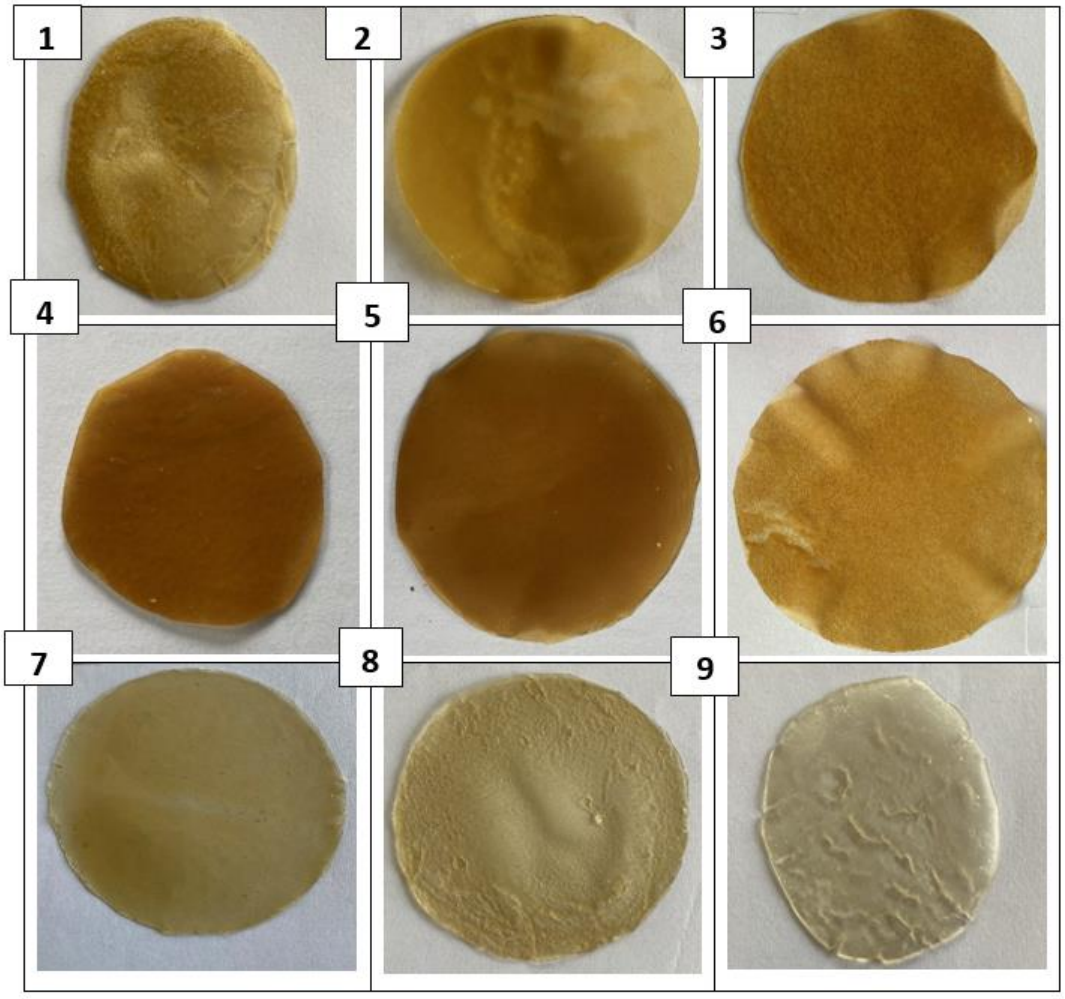

Fig. 3.3: Appearance of Potato starch (PS)-casein blended film

(PS: Casein ratios as: 1) 10:90, 2) 20:80, 3) 30:70, 4) 40:60, 5) 50:50, 6) 60:40, 7) 70:30, 8) 80:20, 9) 90:10)

Table 3.8 Thickness, Solubility, and, Water Vapor Permeability of PS-based films

Starch films	Thickness(mm)	Solubility (%)	WVP (g mm/m^2/h/kPa)
NPSF	0.14±0.02^a	20.50±0.88^a	1.31±0.40^a
ANNF	0.13±0.01^a	17.31±1.31^b	0.65±0.09^b
HMTF	0.13±0.01^a	13.57±1.00^c	0.20±0.01^b

Values are reported as mean ± standard deviation of three replications. Means followed by the same superscript small letters within a column are not significantly different ($p<0.05$). (NPSF-Native PS films), ANNF- Annealed starch films, HMTF- Heat-moisture treated starch films)

Table 3.9 Thickness, Solubility, and Waer Vapor Permeability of casein-based films

Starch films	Thickness(mm)	Solubility (%)	WVP (g mm/m^2/h/kPa)
NCF	0.27±0.013^a	19.30±0.88^a	0.673±0.40^a
ATF 15	0.274±0.012^a	17.90±1.31^b	0.346±0.09^b
ATF 30	0.284±0.007^a	17.65±1.00^b	0.384±0.01^b
UTF 15	0.318±0.002^a	15.54±1.00^c	0.375±0.0023^c
UTF 30	0.302±0.006^a	14.95±1.00^c	0.357±0.001 ^{d}

Values are reported as mean ± standard deviation of three replications. Means followed by the same superscript small letters within a column are not significantly different ($p<0.05$), NCF- Native Casein, UTF- ultrasound treated casein, ATF- Autoclave treated casein.

T**able 3.10** Characteristics of PS and casein blended film

Parameters	30:70	40:60	50:50	60:40	70:30
Thickness (mm)	0.383±0.03^b	0.34±0.02^a	0.42±0.18^c	0.46±0.002^d	0.49±0.006^e
Solubility (%)	13.25±0.35^e	15.57±1.00^c	13.89±0.43^c	17.31±1.31^d	20.50±0.88^e
WVP (g mm/m^2/h/kPa)	1.31±0.004^a	0.65±0.09^d	0.54±0.01^e	1.13±0.0023^c	1.20±0.001^b

Values are reported as mean ± standard deviation of three replications. Means followed by the same superscript small letters within a column are not significantly different ($p<0.05$).

3.3.3.2. Solubility

According to Dutta and Sit (2023), water resistance and instant water solubility are crucial factors in developing biodegradable or edible films for food preservation, particularly when films contact water or serve as product coatings. Significant variations ($p<0.05$) in solubility emerged between native and modified films. Higher solubility generally indicates reduced water resistance. As shown in Table 3.8, native PS films demonstrated higher water solubility compared to ANNF and HMTF variants. Solubility values were highest in NPSF (20.50%), followed by ANNF (17.31%) and HMTF (13.57%). These results aligned with Colla et al.'s (2006) findings for amaranth film (approximately 15.20% solubility). The reduced solubility in modified starch-based films suggests potential applications: HMTS and ANNS modifications could be suitable for packaging cakes, candies, bread, or as confectionery coating materials. Conversely, the higher solubility of NPS-based films makes them appropriate for fruit and vegetable coatings, given their washability, as noted by Luchese et al. (2015). Similarly, native casein-based films were highly water-soluble compared to ultrasound and autoclave-treated casein-based films presented in **Table 3.9**. Higher solubility shows decreased water resistance. Enhanced solubility (19.30%) was seen in NCF followed by ATF 15 (17.90 %), and ATF 30 (17.65 %). Ultrasound-treated casein biofilms showed lower solubility values of UTF 30 (15.54%) and UTF 15 (14.95%). The heat treatment of the film-forming mixture had a substantial impact on solubility. In comparison to native casein films, autoclave-treated films posed a considerably decreased water solubility. The water solubility values of autoclave-treated films were comparable to those observed by Ramos et al. (2013) and Silva et al. (2018) for whey-protein and pullulan-based films. Heat-denatured whey proteins become more insoluble in films due to intermolecular disulfide linkages, but unheated whey proteins create soluble films (Wang et al., 2019). According to some authors, the application of ultrasonic exposes the hydrophilic protein groups outside the molecules, resulting in some degree of hydrolysis (Jambrak et al., 2009; Wu et al., 2018; Tian et al., 2020). **Table 3.10** additionally showcases the solubility differences among various film compositions. Films made of pure starch and pure casein displayed higher solubility while blending notably decreased film solubility (Dutta and Sit 2022, 2023). Starch-based films exhibited high water solubility, with increased solubility corresponding to higher PS concentrations. The decline in solubility for the blends might be attributed to cross-linking, forming hydrogen bonds that limit hydroxyl group

availability for interaction with water molecules (Jain et al., 2018). Among the developed films, the 70:30 PS: casein ratio showed the highest solubility (20.50%), followed by the 60:40 PS: casein ratio (17.31%). Films developed at a 50:50 PS: casein ratio displayed lower solubility (15.57%). The addition of casein notably reduced solubility, with increased casein concentration insignificantly affecting or slightly decreasing solubility (Basiak et al., 2017). Starch (PS) with its highly polar structure, displayed higher water solubility compared to globular proteins. Ultrasound treatment of caseins contributed to reduced film solubility, while heat treatment of PS during film production exposed hydrophobic groups, enhancing solubility. Conversely, ultrasonic conditions stretched casein molecules, fostering a compact network structure that reduced film solubility by enhancing PS-casein interaction (Liu et al., 2021). Similar changes in solubility were observed in previous investigations involving native and oxidized PS biodegradable films (Fonseca et al., 2018; Yang et al., 2019).

3.3.3.3. Water vapor permeability

Water vapor transmission, indicating moisture transport through films, is crucial for food packaging as it affects product quality by controlling water adsorption and desorption (de Moraes Crizel et al. 2017). **Table 3.8** presents WVP values for PS films. The low permeability of PS films correlates with wettability and moisture intake, also relating to reduced amylose content (Calva-Estrada et al. 2019). Since limiting moisture transfer between food and the environment is essential for food packaging, minimal WVP is desirable. WVP values ranged from 0.20 to 1.31 g mm/m²/h/kPa. HMT-modified PS films showed the lowest WVP (1.31 g mm/m²/h/kPa), while ANN films exhibited intermediate values (0.65 g mm/m²/h/kPa), and NPSF demonstrated the highest WVP (1.31 g mm/m²/h/kPa) as shown in **Table 3.8**. These values exceeded those reported by Araujo-Farro et al. (2010) for quinoa starch film (0.204 g mm/m²/h/kPa). Niu et al. (2021) attributed the modified bio-films' reduced WVP to intermolecular hydrogen bonding between glycerol and starch matrix, resulting in stronger interfacial adhesion and lower solubility with enhanced water resistance. Crystallinity percentage also influenced WVP, as demonstrated by Zhang et al. (2018), who reported the lowest WVP (789.41 g/m²/d) in PS films containing 100 nm nano-SiO_2 crystals, attributed to decreased crystallinity. The WVP of casein-based films were shown in **Table 3.9**. The values of WVP ranged from 0.357 to 0.673 g mm/m^2/h/kPa. Ultrasound-treated film (UTF) represented lower WVP

values (UTF 30- 0.357 g mm/m^2/h/kPa and UTF 15 0.375 g mm/m^2/h/kPa) while autoclave-treated films (ATF 30 0.384 g mm/m^2/h/kPa and ATF 15 0.346 g mm/m^2/h/kPa) with native casein films depicting greater WVP value (0.673 g mm/m^2/h/kPa). The main benefit of higher water vapor permeability is the protein-based films' increased solubility (Mihalca et al., 2021). Following Abral et al. (2019), the denser polymer structure in ultrasonicated films caused a stronger resistance to the passage of water molecules, which led to a decline in the films' WVP values. Decline in WVP occurred as the duration of the ultrasonication increased (Asrofi et al., 2018). Biopolymer-based films' moisture barrier abilities can be improved by ultrasonication used for a sufficient amount of time (Mi et al., 2021). Cruz-Diaz et al. (2019) examined the properties of heat, ultrasonic, and/or transglutaminase-treated whey protein edible films. The outcomes revealed that compared to samples merely treated with transglutaminase or heat treatment, the lower WVP values of the films treated with ultrasound were seen. This is considering ultrasound that enhances the emulsifying abilities of whey protein, which leads to improved lipid film distribution. Permeability values reduced compared to those observed in whey protein films that had been heated or subjected to ultrasound treatment as reported by Banerjee et al. (1996), that were 10.6 and 12.4 g mm/kPa m^2, respectively, including the heat-treated WPI films values (1.5–5.0 g mm/kPa m^2) depicted by Jooyandeh (2011). Film WVP reduces when lipid concentration rises, but as emulsion particle size drops, the impact gets increases (Cruz-Diaz et al., 2019). The WVP results, detailed in **Table 3.10** and represented in **Fig. 3.4**, demonstrate a range between 0.54 and 1.31 g mm/m²/h/kPa for films prepared using blends of PS and casein across various proportions. These results are compared to films made of pure starch and pure casein. Notably, **Fig. 3.4** illustrates the differences, showing a general reduction in WVP in the blends of PS and casein, indicating favorable film characteristics. The use of different proportions of PS and casein led to varying WVP values. Specifically, films with a 50:50 proportion displayed the lowest WVP value (0.54 g mm/m²/h/kPa), while those with proportions of 70:30 exhibited higher values (1.20 g mm/m²/h/kPa). Films with a 30:70 proportion recorded the highest values (1.31 g mm/m²/h/kPa). This trend suggests that increased protein concentration correlates with decreased WVP, whereas higher starch concentrations are associated with higher WVP values. Additionally, the addition of starch in different proportions contributed to increased WVP values. The varied gradients highlighted the relationship between WVP and the films' composition and plasticization used to measure average moisture levels during the stationary permeation state. This differentiation allowed for an understanding of

permeation behaviors based on film composition and plasticization (Basiak et al., 2017). Moreover, the reduced WVP observed in bioactive films was attributed to the presence of polyphenolic groups (hydroxyl) within the extract, leading to crosslinking with proteins and polysaccharides (More et al., 2022). Specifically, the low WVP observed in the 50:50 starch-protein blend emphasizes its effectiveness as a barrier, consequently extending the shelf-life of food products. Supporting these findings, various studies have noted a tendency for starch and protein composite films to decrease in WVP within film-forming solutions (Shojaei et al., 2019; Sukhija et al., 2019).

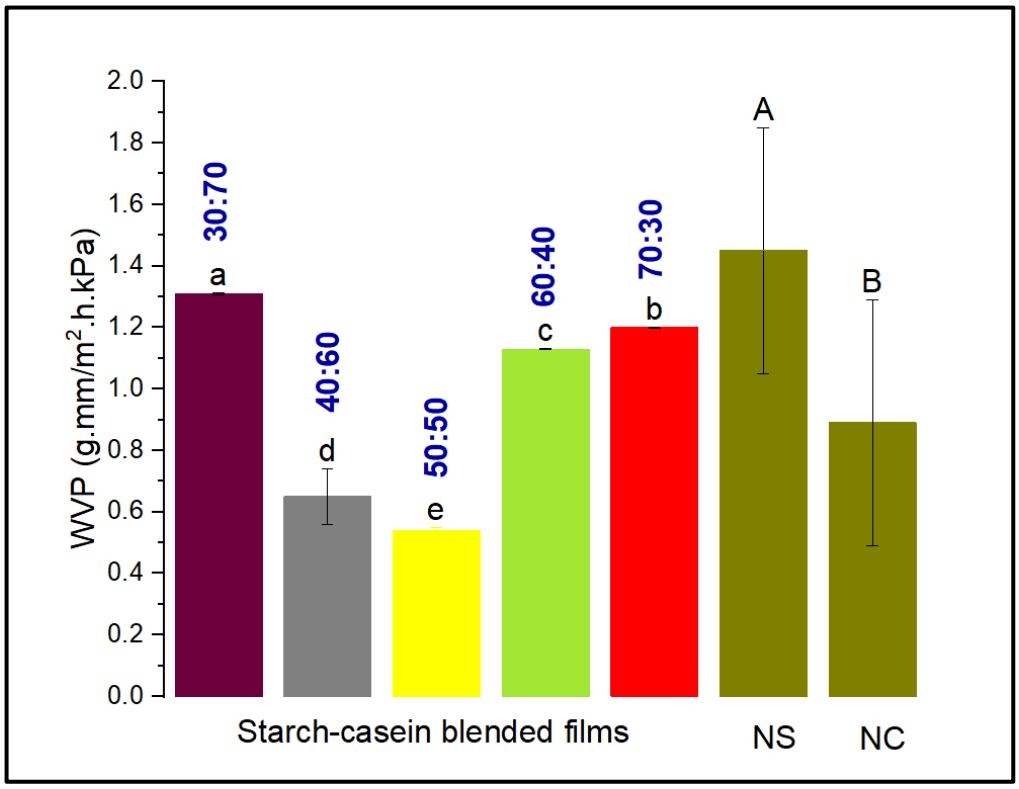

Fig. 3.4 Water vapor permeability of PS and casein blended film (NS- native starch, NC- native casein)

3.3.3.4. Film color and optical properties

Color represents a vital visible characteristic in food packaging films, with starch-based film color parameters presented in **Table 3.11**. All films exhibited transparency. PS films showed consistent L* values (46.476 to 47.856), with no significant differences in a* and b* parameters among samples **(Table 3.11)**. These color values exceeded those reported by Araujo-Farro et al. (2010) for quinoa starch. The films demonstrated positive a* (1.03 to 1.11) and b* (3.49 to 3.73) values, indicating redness and yellow tendencies.

Color characteristics are influenced by starch source, amylose-to-amylopectin ratio, and granular configuration. Film opacity is particularly significant for food surface coating applications. Film transparency correlates inversely with opacity values, with increased thickness generally resulting in greater opacity. As demonstrated by Mali et al. (2005) in yam starch bio-films, thicker films appear more opaque. PS-based films, both native and modified, showed opacity values ranging from 1.15 mm^{-1} to 3.70 mm^{-1} **(Table 3.11)**. Basiak et al. (2017) noted that starch source influences bio-film opacity and transparency; PS films are typically transparent, while corn and wheat starch bio-films appear opalescent. NPSF exhibited greater thickness and consequently higher opacity compared to ANN and HMT variants. Modified films (HMTF and ANNF) demonstrated lower opacity values than NPS films, correlating with their thickness. As Woggum (2014) indicated, higher opacity values signify reduced transparency. Native PS films showed the highest opacity (3.70 mm^{-1}), appearing more opaque than modified variants. Modified films demonstrated significantly lower opacity than native starch-based films ($p<0.05$), an important consideration for packaging applications. Farris et al. (2009) noted increasing industry focus on transparent films due to growing consumer demand for see-through packaging. Consequently, transparency (low opacity) becomes crucial for films intended as food surface coatings where package visibility is desired. For caseinate films, L* (lightness) data ranged from 76.21 to 88.94, a* (redness) data ranged from 2.22 to 6.70, and b* (yellowness) varied from 18.41 to 25.05 values presented in **Table 3.12**. In optimal conditions for ultrasonic treatment, high-quality color characteristics can be achieved as for color coordinates for casein. The redness a* value increased after modification although significantly decreased in L* value. Yellowness (b*) values increased upon alterations of ultrasound and autoclave, which may be due to caseinate effects. The opacity values increased upon modification for casein-based films that varied from 0.72 mm^{-1} to 2.96 mm^{-1}. Higher opaque films often have enhanced barrier properties against moisture and gases. This is vital for preserving the integrity of the packaged goods, especially for hygroscopic materials that can absorb moisture and deteriorate. This combination of functionality and visual appeal makes high-opacity films a valuable choice in the packaging industry (Guzmon-Puyol et al., 2022). Additionally, color parameters exhibited significant variation ($p<0.05$) across the various developed proportions of starch-casein blends. **Table 3.13** presents the color attributes for starch and protein blended films. Regarding lightness, an increase in starch concentrations (70:30) in the developed starch-casein proportionate films yielded higher lightness values. The films with equal

proportions of starch and protein (50:50) displayed a lightness value of 68.49. Conversely, higher casein concentrations resulted in lower lightness values, with measurements at 76.93 and 75.04, showcasing that higher starch concentrations correlated with increased lightness. Notably, the 70% starch and 30% casein proportion exhibited a value of 80.87 for lightness, indicating film transparency. The a* parameter showcased negative values ranging from -0.33 to -0.8 across five different proportionate films, suggesting a shift in film color towards green hues. Comparing b* values, pure starch films, films with a 50% starch and 50% protein ratio, and pure protein films displayed similar levels at 2.90, 27.08, and 3.92, respectively (Dutta and Sit, 2022, 2023). However, starch and casein blends with ratios of 30:70 and 40:60 exhibited considerably higher values than both pure starch films and those with a 50:50 ratio. The total color difference value (ΔE) ranged from 16.82 to 37.57. Similar to the b* coefficient, ΔE values portrayed a consistent trend across pure starch films, 50:50 ratio films, and pure protein films. Notably, samples containing 60% starch and 40% protein, as well as 40% starch and 60% protein isolate, displayed notably higher values. Thus, the incorporation of casein and PS led to a reduction in the L* value and an increase in both a (redness), b (yellowness), and ΔE values in the composite biodegradable film (Huntrakul et al., 2020). The findings align with Galus and Kadzińska (2016) comparative study on alginate/pectin films, which highlighted a significant increase in ΔE with higher starch and protein content. This correlation resonates with the development of composite biodegradable packaging materials by Sukhija et al. (2016). The film exhibited a more yellowish hue due to the addition of casein. However, the yellowness appeared to diminish with increased concentrations of PS, a consistent observation supported by visual analysis. Sun et al. (2013) suggested that the yellow coloration attributed to protein-aldehyde interaction stemmed from intermediate or final products of the Maillard reaction. To evaluate UV transmission properties and their potential impact on film quality, a transmittance curve was generated. **Fig. 3.5 and Table 3.14** illustrate the light transmission curve of starch and protein blended films, showcasing variations in transmittance (% T) across the 200 to 800 nm spectrum. The blended films, prepared at differing ratios, exhibited lower light transmittance, decreasing as the casein ratio increased. PS films displayed high transparency, whereas increased protein concentrations notably reduced light transmission, especially in the UV range from 200 to 800 nm. The % transmittance of the developed films increased proportionally with the wavelength. Structural differences between starch and protein components likely contributed to the observed variations among different proportions of starch and protein

(Lin et al., 2019). The aggregation of casein molecules led to a rougher film surface near the isoelectric point (Khoshkalampour et al., 2023). Films crafted with a 50:50 proportion of starch and casein displayed reduced light absorption across wavelengths. Furthermore, the interaction of casein with PS and glycerol altered the refractive index of the blended films, consequently decreasing their transmittance (More et al., 2022). Similarly, other proportionate blended films demonstrated comparable % T, potentially indicating increased flexibility of starch chains within amorphous granule regions and reduced light absorption (Wang et al., 2017). Higher pH levels prompted casein molecules to transition from a spherical to a chain shape, resulting in a more ordered structure, and facilitating light passage through the blended films (Yang et al., 2019). Conversely, higher concentrations of PS films displayed heightened light transmission due to the reorganization of components, including the movement of plasticizers released from the material (Lin et al., 2019). Notably, the 50:50 starch-casein developed films demonstrated lower UV-visible light transmission, suggesting a stronger UV barrier property, potentially attributed to casein's light absorption and scattering capabilities. Additionally, protein influenced the crystallization of PS in the film, inducing surface roughness that led to light dispersion and gloss reduction. Overall, PS films were transparent and colorless, while blended films with lower light transmittance were deemed desirable for food systems as they could mitigate light-induced lipid oxidation (Liu et al., 2021; Lin et al., 2019). Research on starch-protein interactions and their influence on the physicochemical and digestible properties of blends was conducted. The results are in agreement with the lower transmittance findings of Huntrakul et al. (2020) and Liu et al., (2021).

Table 3.11 Color properties of native and treated PS-based films

Starch	L*	a*	b*	Opacity (mm^{-1})
NPSF	47.856±1.14[a]	1.05±0.08[a]	3.67±0.27[b]	3.70 ± 0.23[a]
ANNF	47.656±1.06[a]	1.11±0.07[a]	3.73±0.20[a]	1.31 ± 0.13[b]
HMTF	46.476±1.09[b]	1.03±0.04[a]	3.49±0.33[c]	1.15 ± 0.08[b]

(NPSF-Native PS films), ANNF- Annealed starch-based films, HMTF- Heat-moisture treated starch-based films). Values are reported as mean ± standard deviation of three replications. Means followed by the same superscript small letters within a column are not significantly different (p>0.05).

Table 3.12 Color properties of native and treated casein-based films

Casein	L*	a*	b*	Opacity (mm^{-1})
NCF	88.94±0.52[a]	2.22±0.24[d]	18.41±0.43[c]	0.72±0.01[e]
ATF 15	77.33±1.71[b]	6.69±1.13[a]	21.78±0.36[b]	1.04±0.04[d]
ATF 30	78.09±2.90[b]	6.70±0.04[a]	22.20±0.36[b]	2.49±0.23[b]
UTF 15	77.21±0.38[b]	4.52±0.35[c]	25.05±1.24[a]	2.18±0.01[c]
UTF 30	76.21±3.84[b]	5.70±0.75[b]	23.37±1.45[b]	2.96±0.10[a]

NCF- Native casein films, UTF- ultrasound treated casein-based films, ATF- Autoclave treated casein-based films. Means followed by the same superscript small letters within a column are not significantly different (p>0.05

Table 3.13 Color properties of PS and casein blended films

Parameters	30:70	40:60	50:50	60:40	70:30
L*	76.93±1.00[e]	75.04±1.08[d]	68.49±1.15[c]	59.16±0.68[b]	80.87±0.56[a]
a*	-0.60±0.09[c]	-0.75±0.20[a]	-0.48±0.05[d]	-0.8±0.0002[a]	-0.33±0.001[d]
b*	17.68±0.28[c]	29.60±0.11[a]	27.08±0.27[b]	17.16±0.08[c]	12.27±0.32[d]
ΔE	17.94±0.38[d]	34.13±0.18[c]	36.07±0.88b	37.57±0.62a	16.82±0.54[e]

Means depicted by different superscript small letters within the column are significantly different ($p<0.05$).

Table 3.14 Light transmission of PS and casein blended films

Film samples	Light transmission across wavelengths (nm)						
	200	**280**	**350**	**400**	**500**	**600**	**800**
30:70	1.403	33.586	47.986	49.841	52.850	54.216	56.866
40:60	3.297	22.920	46.807	54.394	56.653	56.653	60.619
50:50	2.095	22.183	27.814	29.564	30.529	35.319	37.317
60:40	1.685	30.446	53.997	44.537	47.269	48.793	51.684
70:30	1.854	37.109	41.765	48.149	50.292	51.618	54.588

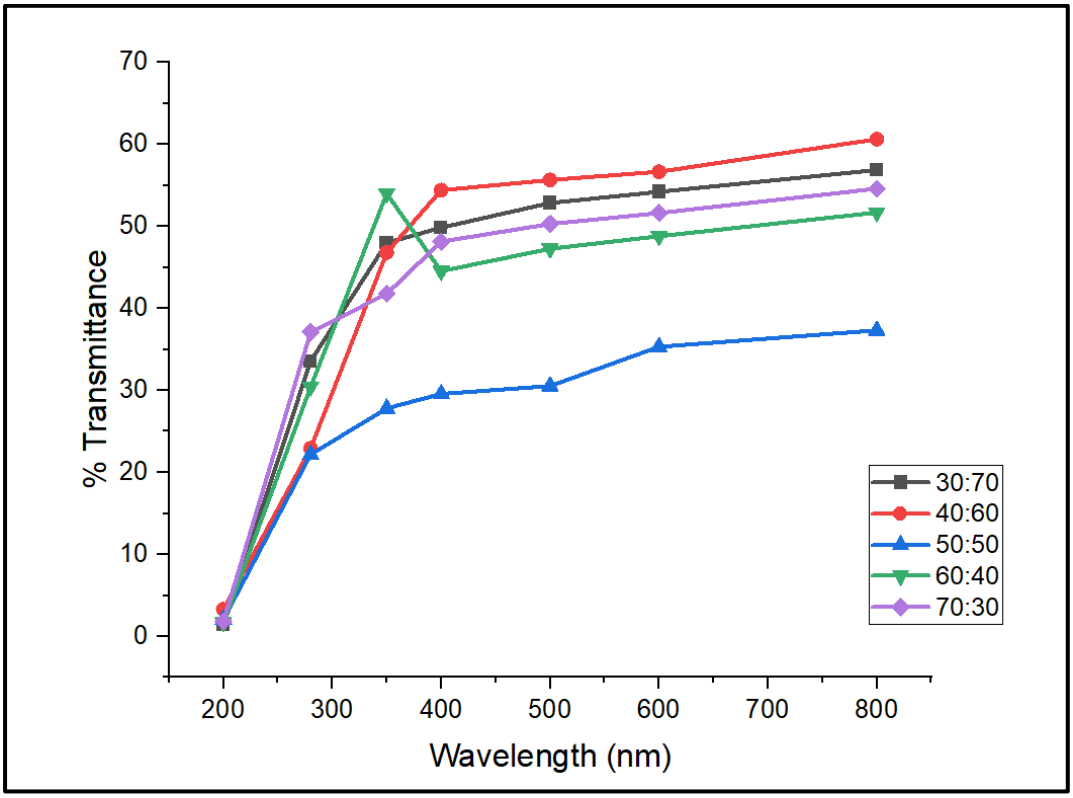

Fig. 3.5 Light transmittance curve of PS and casein blended film

3.3.3.5. Mechanical properties

Tensile strength (TS) and elongation percentage (EAB%) measurements evaluate the relationship between film mechanical properties and chemical structure. As noted by Lourdin et al. (1995), these characteristics depend on polymeric chain packing, chain interactions, and film thickness, which environmental relative humidity significantly

influences. Tensile strength represents the maximum tensile force generated during tension analysis. **Table 3.15** shows significant variations ($p<0.05$) in PS films' mechanical properties. HMT starch films demonstrated the highest TS at 7.62 MPa, with HMT treatment requiring 3.941 N puncture force. NPSF exhibited 3.52 MPa TS with 4.86% elongation at break (EAB). According to Hu et al. (2020), native PS film's high molecular weight and sufficient TS contribute to native PS paste's elevated viscosity. HMT films showed superior performance with high TS and 11.36% EAB compared to native and annealed variants. In stress-strain testing, break elongation indicates sample extension from original length at breakpoint, with polymeric substance elongation percentage depending on molecular chain flexibility. ANNF showed 4.24 MPa TS and 9.36% elongation at break, exceeding NPS-based films **(Table 3.15)**, indicating greater pliability. Because of the hydrophilic nature of starch films, mechanical traits are substantially affected by the water content, and thus reduced amylose content significantly advances the TS and Young modulus of films manufactured from potato and wheat (Singh et al., 2009). The protein-based film or coating's extensibility and mechanical properties are crucial for maintaining food product integrity during shelf life (Borah et al., 2017). Tensile characteristics of casein-based films showed significant change ($p<0.05$) as shown in **Table 3.16**. Ultrasound-treated casein films showed higher mechanical characteristics compared with autoclave-treated and native casein films. When compared to autoclave-treated casein films and native casein films, UTC 30 films had a greater TS of 9.37 MPa and EAB (%). The TS of native casein-based films was 1.39 MPa with (EAB) % of 4.97%. Modification US 15 possessed TS 8.90 MPa and (EAB) % 9.31. Also, ATF 15 showed a TS of 4.32 MPa with (EAB) % of 8.36 along with ATF 30 which showed a sufficient TS of 5.50 MPa and elongation % of 8.89. Experimental stress-strain curves were used for calculating the blended film's TS and (EAB%) which are shown in **Table 3.17** and **Fig. 3.6 and 3.7**. Pure starch-based films have reported TS of about 3.54 MPa and EAB = 4.86 % while pure casein has reported TS of 1.39 MPa and EAB 4.97 %. The blending of starch and protein has enhanced the mechanical properties. **Table 3.17** shows that the TS of 50:50 proportionate starch-casein blend films was significantly higher ($p<0.05$) (8.62 MPa) among the other proportions. Fonseca et al. (2018) reported similar findings in PS film, noting that increased starch concentration led to granule aggregation and matrix network disruption, reducing film matrix cohesive force. The starch-protein blended films' elongation at break percentages appears in Table 3.17 and Fig. 3.7, ranging from 7.36% to 11.36%. Films with 50:50 proportions showed significantly higher EAB (11.36%)

compared to other ratios ($p<0.05$). Starch/protein addition enhanced blended film flexibility ($p<0.05$). Glycerol plasticizer further improved film flexibility. As Zhuang et al. (2023) explained, glycerol molecules reduce starch compactness, decrease intermolecular interaction, and increase polymer mobility, improving elongation. Higher starch concentrations diminished film thermoplastic properties and elongation percentage, similar to observations in corn starch-collagen composite films (Wang et al., 2017; Kumar et al., 2021). Zhao et al. (2022) reported an enhancement in the mechanical properties of quinoa starch edible films due to the inclusion of quinoa protein. Although the proteins investigated in their study differ structurally from those analyzed in this research, it remains intriguing that proteins, when combined with starch, generally seem to positively impact the strength and flexibility of films, as observed in our findings.

Table 3.15. Mechanical Properties of PS-based Films

Starch Films	Tensile Strength (MPa)	Elongation at break (%)	Sealing Strength (MPa)
NPSF	3.54 ± 0.73^{c}	4.86 ± 0.81^{b}	3.05 ± 0.15^{b}
ANNF	4.24 ± 0.67^{b}	9.36 ± 1.04^{a}	3.85 ± 0.92^{ab}
HMTF	7.62 ± 1.44^{a}	11.36 ± 0.50^{a}	4.06 ± 0.26^{a}

Means followed by the same superscript small letters within a column are not significantly different *($p>0.05$)*. NPSF-native Ps films, ANNF-annealed films, HMTF- Heat-moisture treated films

Table 3.16. Mechanical Properties of casein-based films

Starch Films	Tensile Strength (MPa)	Elongation (%)	Sealing Strength (MPa)
NC	1.39 ± 0.73^{e}	4.97±0.81e	2.35 ± 0.15^{b}
ATF 15	4.32 ± 0.67^{d}	8.36±1.04d	2.85 ± 0.92^{ab}
ATF 30	5.50 ± 1.44^{a}	8.89±0.50c	3.06 ± 0.26^{a}
UTF 15	8.90±0.21	9.31±0.50b	3.97 ± 0.23^{a}
UTF 30	9.37±1.44	9.87 ± 0.50^{a}	4.23 ± 0.26^{a}

Values are reported as mean ± standard deviation of three replications. Means followed by the same superscript small letters within a column are not significantly different *($p>0.05$)*. NCF- Native casein films, UTF- ultrasound treated casein-based films, ATF- Autoclave treated casein-based

Table 3.17. Mechanical properties of PS and casein blends

Parameters/Blends	30:70	40:60	50:50	60:40	70:30
TS (MPa)	3.62±0.73^{e}	4.24±0.67^{d}	8.62±1.44^{a}	6.32±0.21^{c}	7.86±1.44^{b}
E (%)	8.86±0.81^{c}	9.36±1.04^{b}	11.36±0.50^{a}	6.87±0.35^{e}	7.36±0.50^{d}
Sealing Strength (Mpa)	3.05±0.15^{e}	3.85±0.92^{d}	4.23±0.26^{a}	4.12±0.23^{b}	4.06±0.26^{c}
Sealing efficiency (%)	118.68±0.15^{e}	110.12±0.15^{e}	203.78±0.15^{e}	153.39±0.15^{e}	193.59±0.15^{e}

Values are reported as mean ± standard deviation of three replications. Means followed by the same superscript small letters within a column are not significantly different ($p>0.05$).

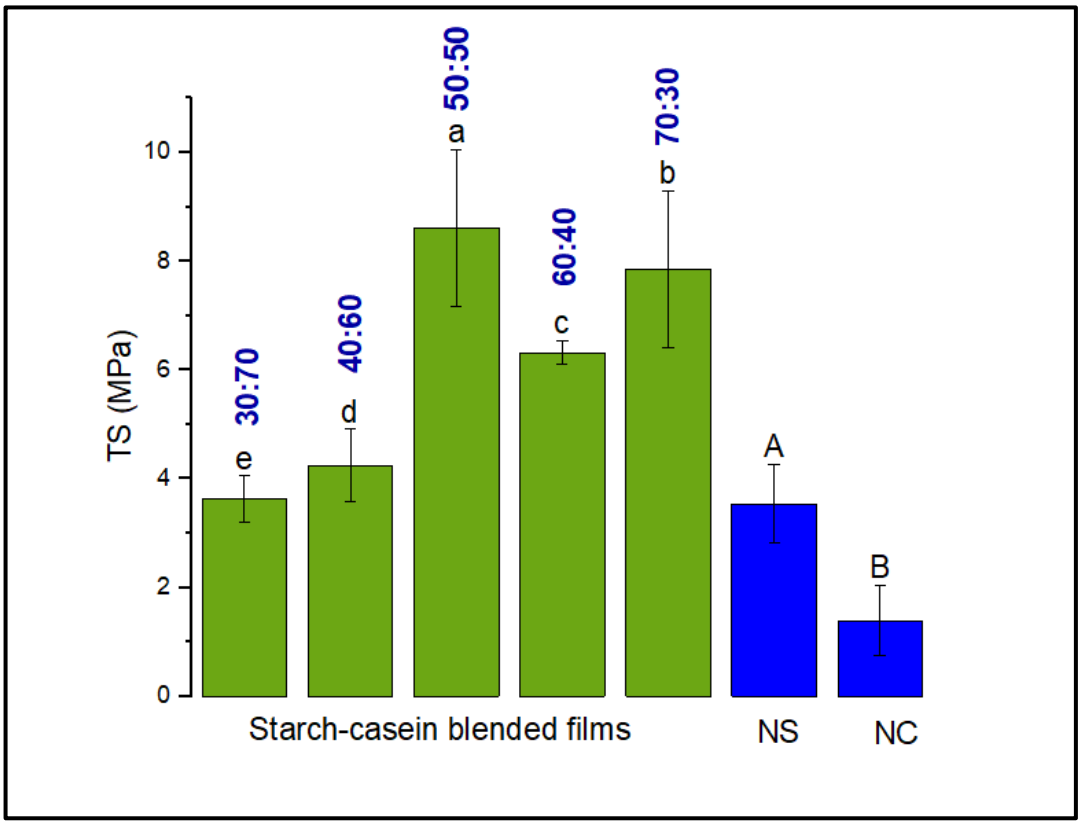

Fig. 3.6 Tensile strength (TS) of PS and casein blended film in comparison with NS: Native starch and NC: Native casein

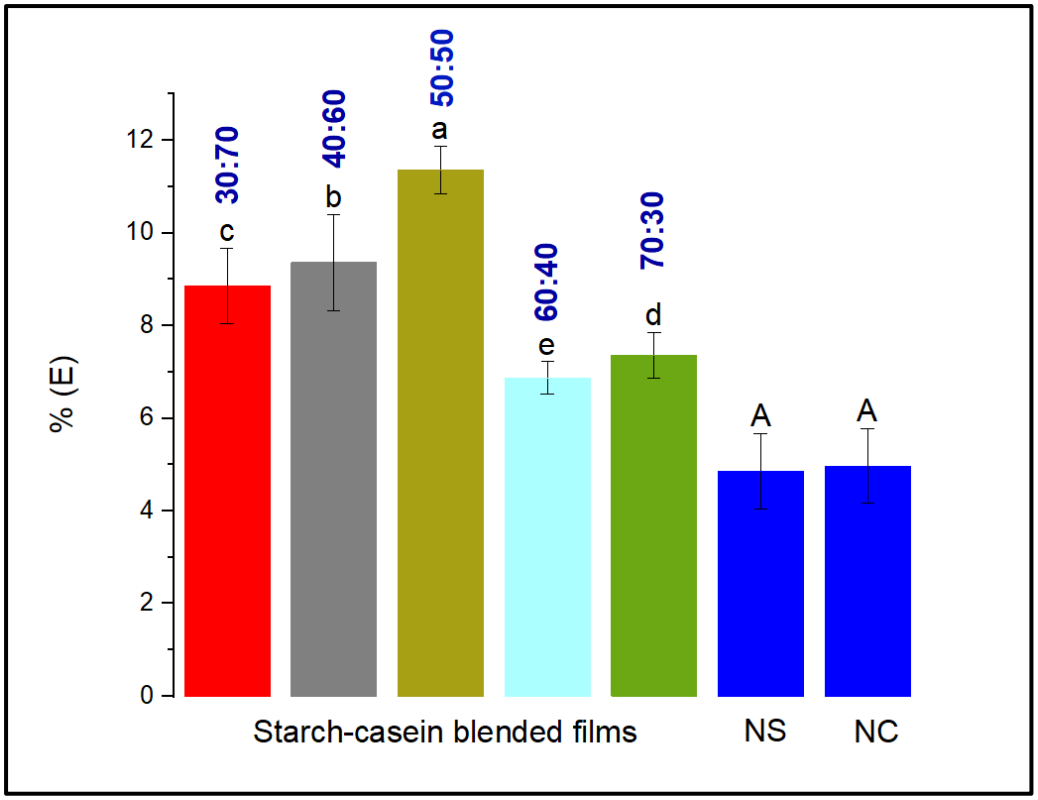

Fig. 3.7 Elongation at break (E%) of PS and casein blended film in comparison with NS: Native starch and NC: Native casein

3.3.3.6. Sealing properties

One of the key requirements for polymeric films used in the creation of flexible packaging is heat sealability. The quality of the seal is determined by its strength. When heat is supplied during film sealing, mass diffusion between the molten layers creates simultaneous interfacial contact, which causes the polymers to melt. On cooling down, inter-diffusion causes the tangling of polymers across melted layers, resulting in a stiff joint. The heat sealability trait of packaged film forms an important consideration for application in the production of pouches (Das and Chowdhury, 2016). Ensuring films possess adequate thermo-sealability and seal strength is crucial to prevent package malfunction and spillage of contents (Liu et al., 2020). Without the use of an external solution, starch-based films were first bound by their adhesive qualities and heat, demonstrating adequate seal strength. The PS-based film's seal strength is shown in **Table 3.15**. When the two layers of film separate at the interface and the seal region remains intact, but the film rips at the edge of the sealing part, the tearing mode failure was determined in order to assess the packing performance. Failure in the tear mode indicates a stronger seal. The maximum seal strength of 4.06 MPa was demonstrated by modified

HMT films. Films made from annealed starch have a suitable 3.85 Mpa seal strength. The seal strength of native starch films was 3.05 MPa, indicating a lower seal strength. In failure mode, disintegration of polymeric material takes place, enabling two sealed films to simply tear apart (Yuan et al. 2007). Near results were reported by Abdorreza et al. (2011) in which the maximum seal strength obtained was 0.375 N/mm for 0.4 w/w of starch added along plasticizer (sorbitol: glycerol ratio of 3:1). Without employing any external solution, caseinate films showed adequate seal strength. **Table 3.16** represents the seal strength of casein-based film. Modified US 30 films (UTF) exhibited an improved seal strength of 4.23 MPa and UTF 15 depicted a seal strength of about 3.97 MPa. Autoclave-treated casein-based films possessed sufficient seal strength of ATF 30 3.06 MPa and ATF 15 2.85 MPa. Native casein-based films represented a seal strength of 2.35 MPa showing weaker seal strength. The mechanical properties of films are greatly facilitated by ultrasonication. Asrofi et al. (2018) investigated that ultrasound modification duration improved the tensile strength of the films because of the uniform dispersion of additives inside the polymer matrix. The impact of high-intensity ultrasonic modification (20 kHz, 0, 200, 400, and 600 W) on the mechanical characteristics of films made from plum seed protein isolate (PSPI) was investigated by Xue et al. (2018). The authors discovered that the TS value of films treated ultrasonically increased by 85% to 123% when compared to films based on PSPI that had not been treated. These findings suggested that ultrasound modification could improve protein cross-linking during the preparation process, leading to a greater firmer film network (Mi et al., 2021). Tensile strength (TS) and elongation at break (EAB) values of autoclave-treated films were high than those described by Ramos et al., (2013) (TS 0.65-0.75 MPa; EB 18–20%) and Silva et al. (2018) (TS 2.18 MPa; EB 11.24%), most likely as a result of variations in casein protein product properties. Because of improved non-covalent interaction between protein molecules, sonication significantly changed mechanical characteristics (Jambrak et al., 2008). Lipids enhance protein chain mobility and diminish intermolecular attraction forces, increasing the extensibility of films (Chambi and Grosso, 2006). Autoclave treatments also involve a decrease in water content increasing the film's strength including rigidity. When proteins are pretreated with heat, and also when a protein film is heated, the disulfide, hydrogen, and hydrophobic bonding types are increased. As a result, films that have been treated at a higher temperature exhibit a much higher TS (Abdullah-Al-Rahim, 2021). **Table 3.17** and **Fig. 3.18** detail the sealing properties of developed blended films in comparison to pure starch and pure casein films. Compared to pure starch and casein films, sealing

characteristics are enhanced. Said et al. (2021) reviewed studies detailing gelatin-based edible films used in food packaging and observed a similar trend that the addition of materials like starch altered the films' melting point, consequently reducing the energy needed to break the seal. All developed film samples, owing to their uniform thicknesses, exhibited heat sealability. Notable differences in sealability values ($p<0.05$) were observed among the developed films, with the 50:50 starch-casein blended films achieving the highest sealing strength at 4.23 MPa. It's noteworthy that increased concentrations of starch correlated with enhanced sealing strength. The assessment of sealing efficiency revealed variations ranging from 110.12% to 203.78% among the films, with equal proportions of starch and casein blended films displaying the highest sealing efficiency (203.78%) among the developed samples. The 70:30 starch-casein proportionate films also demonstrated sufficient sealability with a sealing efficiency of 193.59%. Sealing efficiency is contingent upon innate capacity. Biobased films with commendable sealing characteristics ensure compatibility with packaging machinery, facilitating efficient and effective packaging processes in manufacturing (Abedinia et al., 2018). These seals act as barriers against external elements such as moisture, air, and contaminants, preserving the integrity and quality of the packaged product. This preservation is particularly critical for extending the shelf life of perishable goods, and preventing spoilage or degradation (Liu et al., 2020). A comparable pattern was noted in the mechanical characteristics: films at this specific tapioca starch: protein ratio appeared to be studied and exhibited greater tensile strength compared to other tested compositions (Izzi et al., 2023) showcasing superior zip quality among all the films examined.

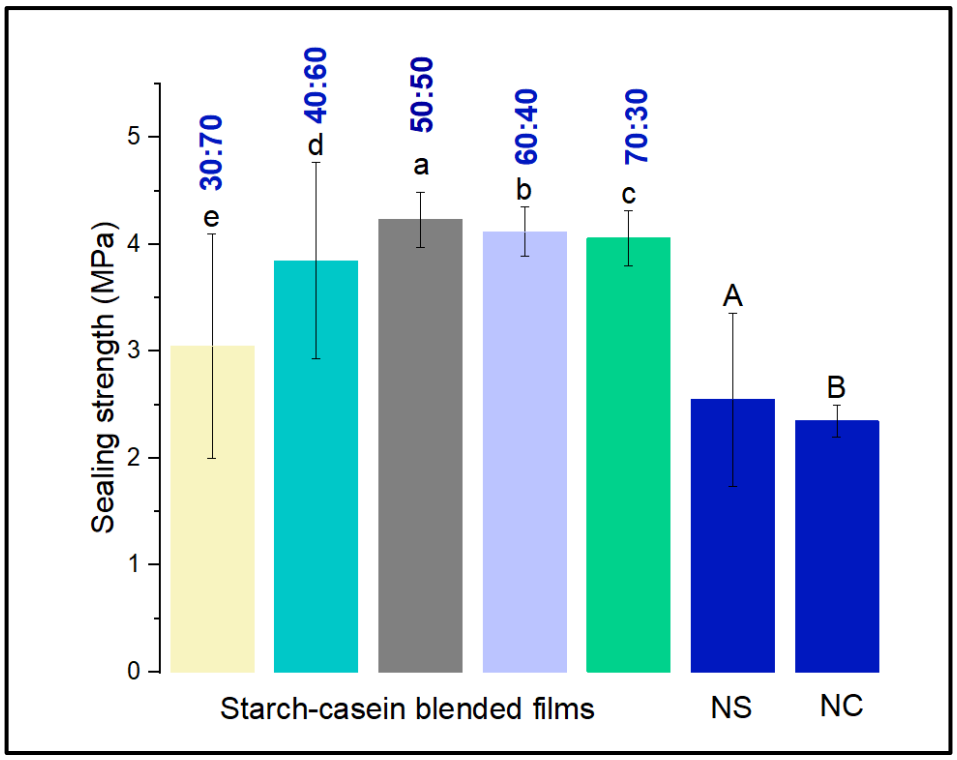

Fig. 3.8 Sealing strength of PS and casein blended film (NS- Native starch, NC- Native casein)

3.3.3.7. Thermal properties

Thermal stability of films is evaluated using thermo-gravimetric analysis (TGA) to determine the maximum functional temperature before biopolymer degradation or property loss occurs (Azevedo et al. 2020). **Fig. 3.9. (A, B, and C)** illustrates thermo-gravimetric curves for native and modified PS films, showing progressive mass loss stages with temperature increase. Initial mass reduction began near 110°C across all PS films due to water evaporation. NPS films exhibited mass changes between ≈110°C and ≈150°C, with a second stage occurring between ≈180°C and ≈210°C. ANN and HMT films showed second and final mass changes from ≈200°C to ≈500°C, while NPS demonstrated final weight loss between ≈300°C and ≈500°C. Iuga et al. (2020) noted that cereal starches' thermal stability improves through amylose-lipid complex formation during HMT. The first phase showed minimal mass loss (approximately 10%) attributed to surface moisture evaporation. Mass degradation between ≈120°C and ≈280°C ranged from 24% to 28% across PS-based films, corresponding to moisture loss and glycerol decomposition. According to Yashini et al. (2024), the third stage indicated thermal expansion with 50%-60% weight loss, likely due to starch matrix de-polymerization and decomposition. Final

weight loss (52%-57%) reflected starch degradation, glycerol breakdown (boiling point 290°C), and product thermal expansion. Modified starch-based films exhibited only two mass loss stages corresponding to starch degradation, attributed to OH group removal and glycosidic linkage breakage. Increased mass losses generally indicate reduced thermal stability, affecting heat exposure performance and durability. These results align with findings from Shi et al. (2013) and Luchese et al. (2015). Azevedo et al. (2020) found similar temperature-dependent mass changes when comparing potato and corn starch thermal resistance. Zhang et al. (2018) noted superior thermo-stability in PS films compared to other starch variants. Increased thermal stability can enhance the performance and durability of films. Results described by de Silva et al. (2018) for cassava starch further support the proposed findings. Additionally, casein protein can be used to make films due to its high heat stability. To form films, casein must melt at high temperatures. **Fig. 3.10. (A, B, C, D, and E)** demonstrated the thermo-gravimetric curves of native and modified casein films where two stages of mass loss were observed, respectively. The figure demonstrates how the thermo-gravimetric mass varied as the temperature rose. Initial mass loss started ≈ at 100℃ in all caseinate films linked to water evaporation. Immediate next mass change took place between ≈110°C and ≈200°C for NC films. In autoclave along with ultrasound-treated films for 15 and 30 mins, the second and last stage mass change occurred at about ≈200°C . 1st phase reported a minimal loss of mass (about 10%) which was due to moisture loss from the film's internal area. Mass degradation around ≈120°C and ≈280°C in all films varied from 50% to 60% denoting thermal expansion in films could be attributed to de-polymerization and glycerol decomposition. Modified casein-based films reported only two stages of mass loss with the last stage corresponding to thermal degradation. After ultrasonic treatment, the film's heat resistance increased. According to numerous studies regarding the thermal characteristics of polymeric films modified with ultrasonication that have been published, ultrasonication increases the thermal stability of the majority of polymeric materials, which in turn affects other physicochemical parameters. As the sonication amplitudes increased from 20% to 30%, the enthalpy improved and the period increased from 10 to 20 mins, which indicated the possibility of reaggregation (Chandrapala et al., 2011; Arzeni et al., 2012).

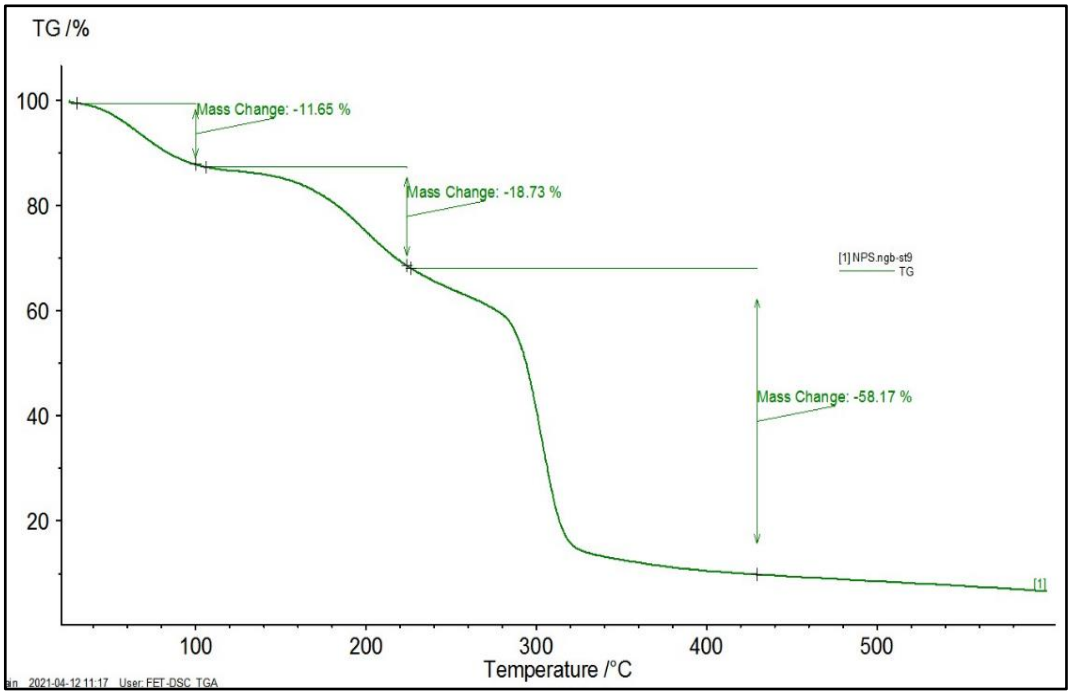

A) Native PS films (NPSF)

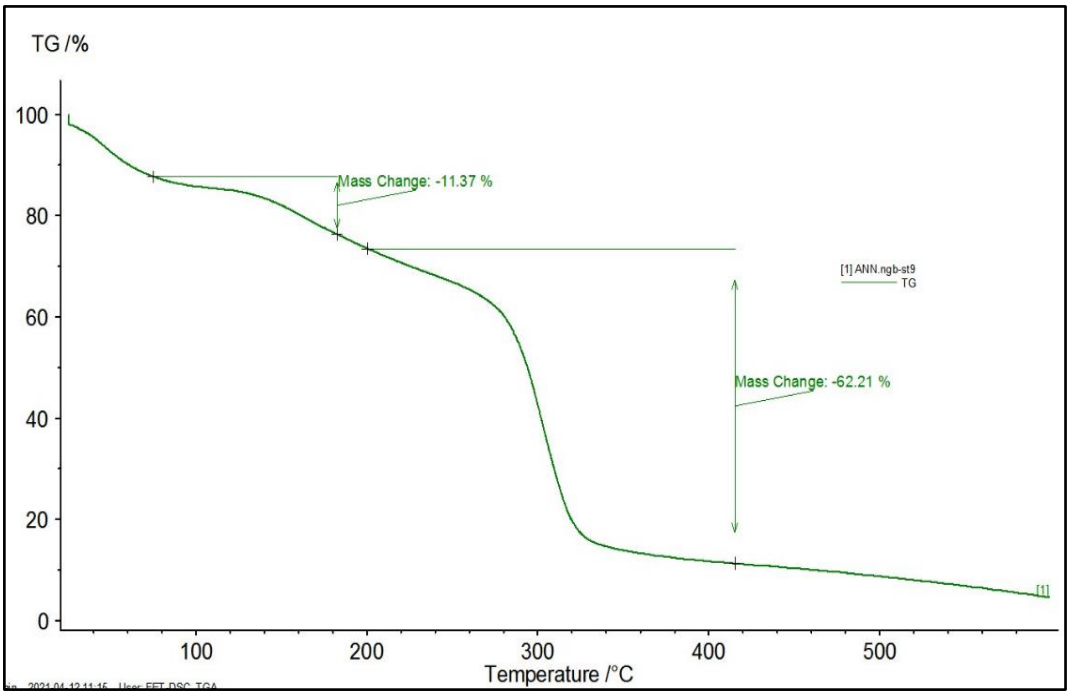

B) ANN-based films (ANNF)

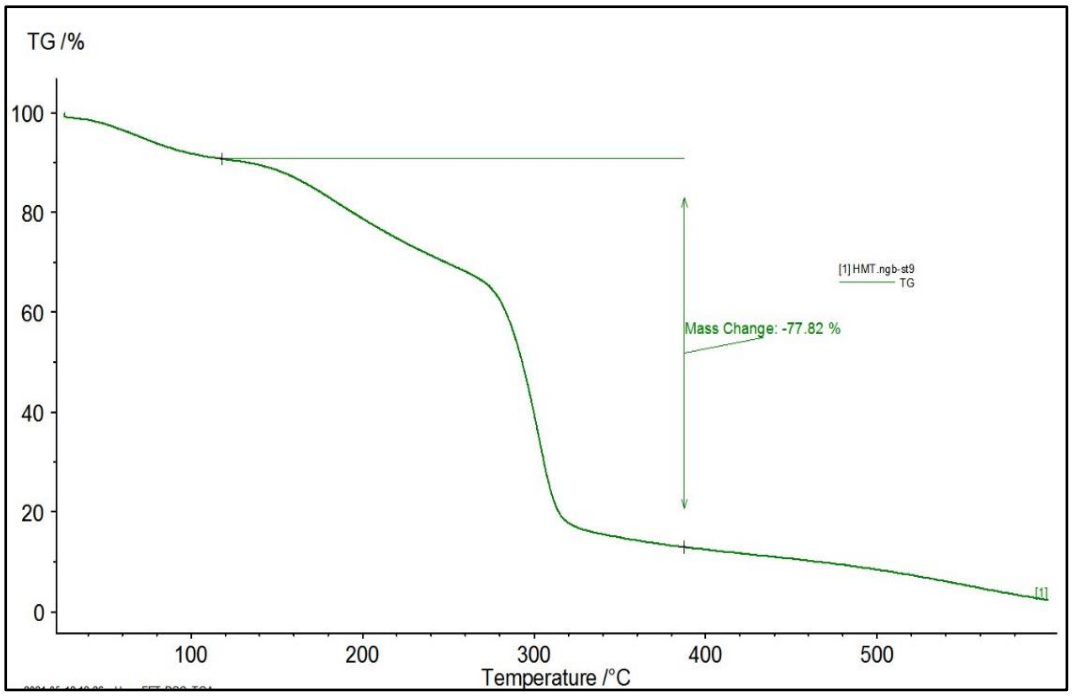

C) HMT-based films (HMTF)

Fig. 3.9 (A, B, C) Thermo-gravimetric Analyses of PS-based films: A) Native-NPSF B) ANNF- Annealed C) HMTF- Heat-moisture treated starch-based films

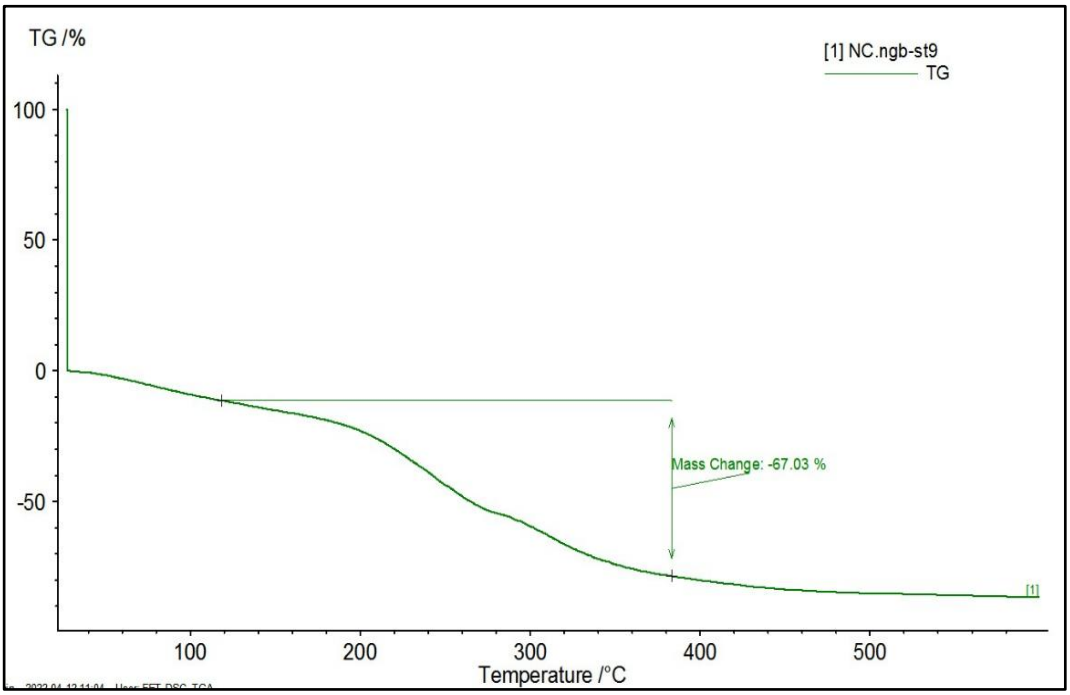

A) NCF

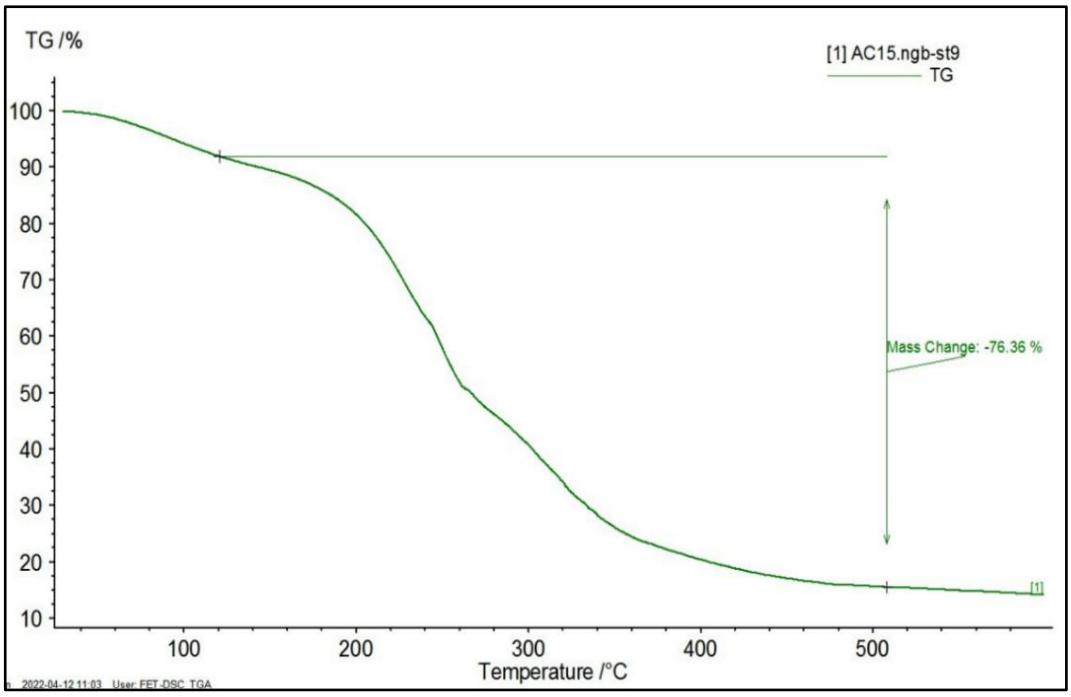

B) ATF 15

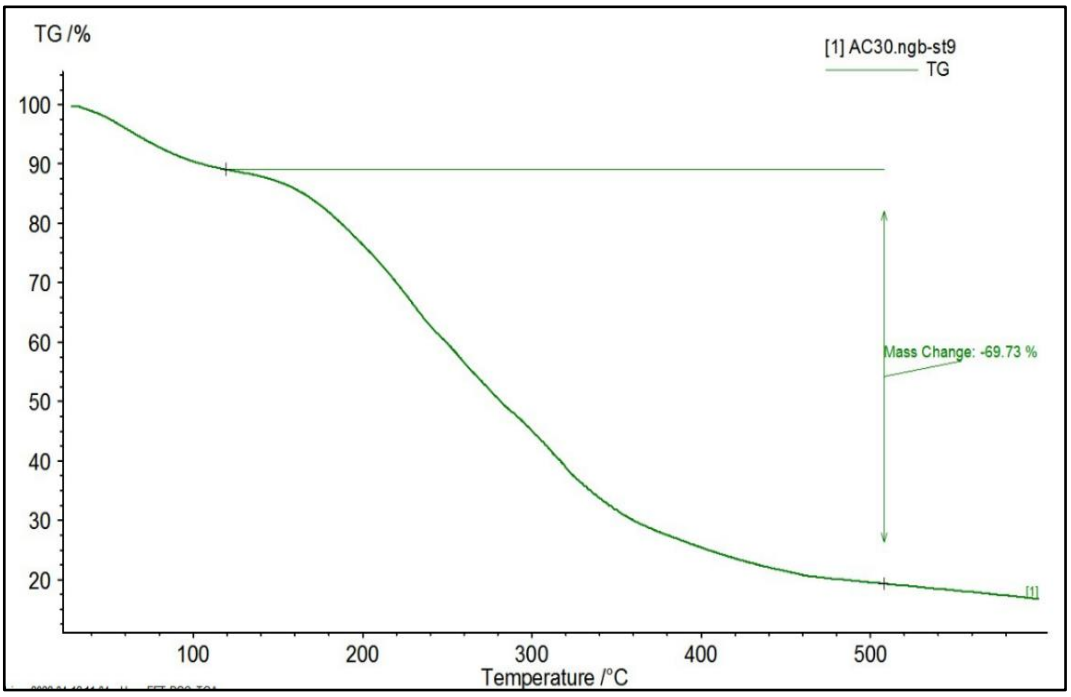

C) ATF 30

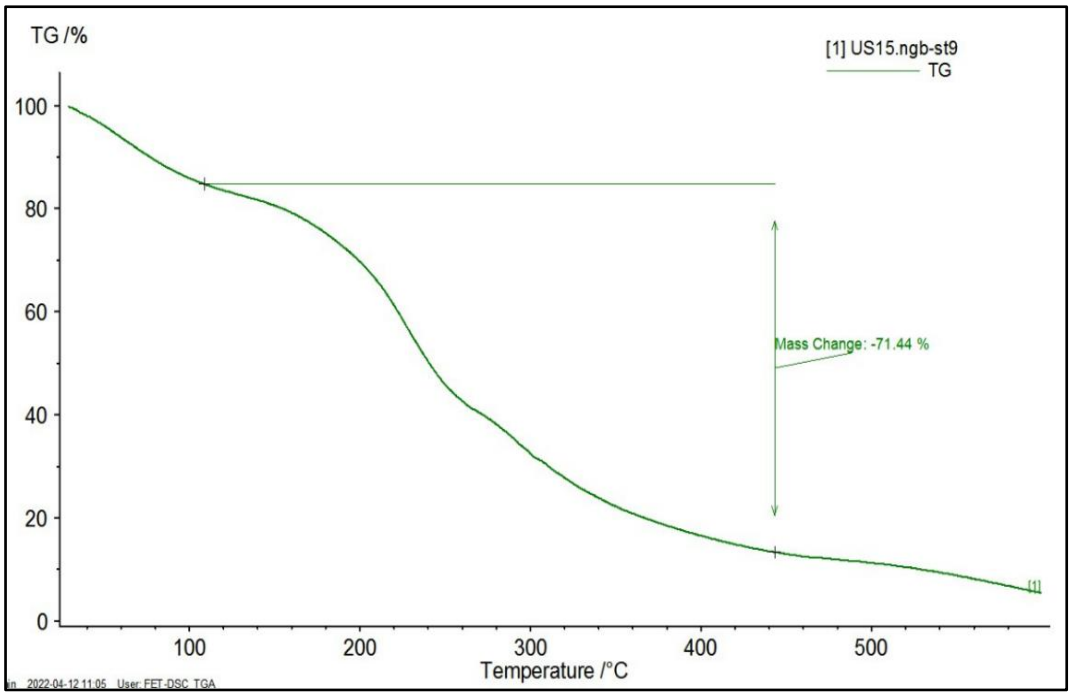

D) UTF 15

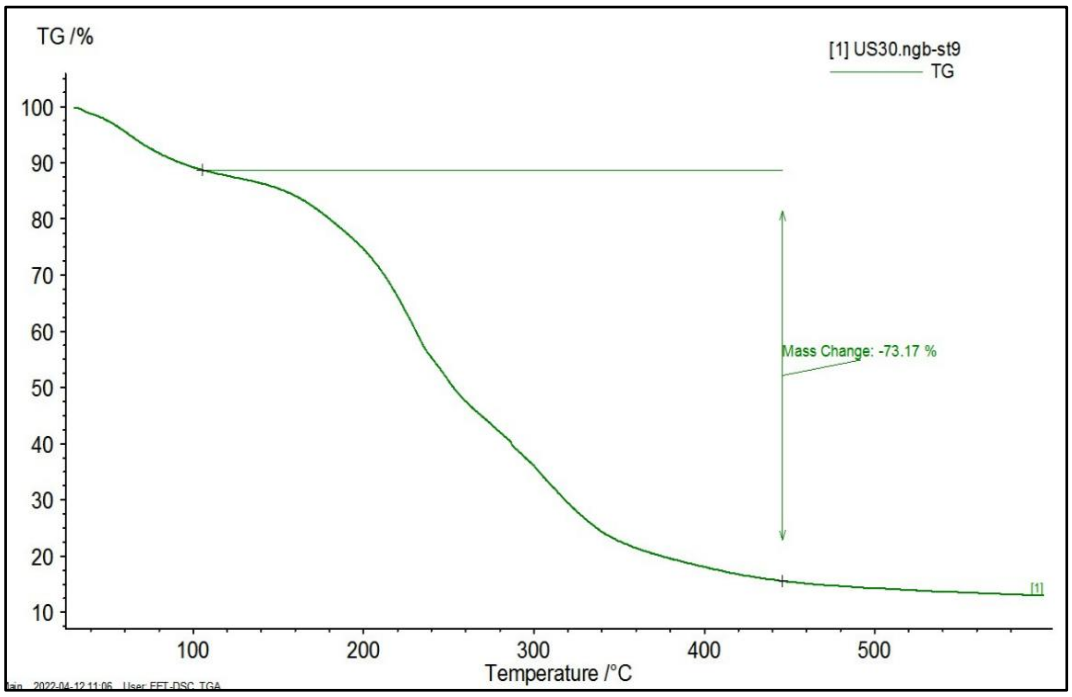

E) UTF 3

Fig. 3.10 (A, B, C, D, E) Thermo-gravimetric Analyses of Casein-based films: A) Native B) AC 15 C) AC 30 D) US 15 E) US 30 (NCF- Native Casein films, UTF- ultrasound treated casein fims, ATF- Autoclave treated casein films)

3.3.3.8. Biodegradability

Visual inspection during their time buried allowed for the observation of the created film's biodegradability. The bio-films' decreased weight led to the final observations. The native and modified starch and casein-based films at the beginning and end of the biodegradability analysis are depicted in **Fig. 3.11**, respectively. PS-based films that decomposed in about 15 days along with casein-based films that got degraded in soil until 12 days, depict that it is suitable from an environmental point of view. The superior biodegradability of casein-based films compared to starch-based films can be attributed to their proteinaceous nature, unique structural properties, effective microbial degradation mechanisms, and hydrophilic characteristics (Yahia et al., 2023). Similar results were demonstrated by Azevedo et al. (2020), who found that bioplastics derived from PS degraded in just 5 days as opposed to about 40 days for bioplastics derived from corn starch. Throughout the analysis period, the degradation areas for both native and modified PS-based show a decrease in the bio-plastic region. PS films showed less resistance to the soil environment. The degradation duration of PS-based films was deemed appropriate when compared to synthetic polymers. The resulting mass changes of starch and casein-based films (native and modified) during the soil burial test are represented in **Tables 3.18 and 3.19**. The weight of three PS-based films and five casein-based films (native and modified) steadily reduced when the exposure duration was extended. It is related to the continual erosion of soil micro-flora (Li et al., 2024). Considering the 50% weight loss, a higher rate of degradation was seen in all the films. The weight loss was 50% after 7 days, indicating a rapid decline. Ultimately, it was found that both the native and treated biopolymeric films adhered to soil particles, which, when touched, broke up into little pieces all over the ground. Because of their improved deterioration potential, the produced films demonstrated decreasing mass loss, which suggests that they will be useful in addressing environmental contamination. The change in mass of the starch-casein blended films, when subjected to soil decomposition, is illustrated in a bar diagram **(Fig. 3.12)**. These films displayed noticeable alterations in their polymer matrix as early as the 2nd week, characterized by the emergence of cracks and tears, reduction in size, color variations, and a distinct crunchy hardness on the surface presented in **Fig. 3.13**. This timeframe likely marked the formation of microbial colonies within the polymer matrix, potentially contributing to the weakening and rupture of the film's polymeric chains (Hirpara et al., 2021). The breakdown happens because microbes feed on and biodegrade

the mixtures, compromising their structural integrity. Water molecules and bacteria occupy the starch areas within the blends, leading to their disintegration. Additionally, the mixtures expanded as they absorbed water during the experiment, which sped up the biodegradation process (Yahia et al., 2023). Upon contact, the films lost their tensile and bending strength, transitioning to a brittle and hardened state—a clear indication of the plasticizer (glycerol) evaporation from the polymer matrix (Mittal et al., 2021). Studies suggest that higher concentrations of hydroxyl (OH), carbonyl (CO), and ester (COOH) groups in starch-based films accelerate their degradation in soil (dos Santos Cotta et al., 2023). This increased presence of functional groups allows greater water penetration within the film's structure, fostering microbial proliferation on the packaging's surface (Su et al., 2023). Moreover, water introduced during degradation interacts with starch molecules' hydroxyl groups, weakening the chemical chains and hastening the biodegradation of packaging materials (Kumar et al., 2021). Visual analysis of the samples revealed that packages composed solely of starch and casein films degraded more rapidly compared to those with proportionate mixtures of casein and starch, resulting in complete degradation by 15 days (Dutta and Sit, 2022). Higher starch concentrations corresponded to faster biodegradation, leading to increased fragility, accelerated mass loss, and heightened microbial presence on the material's surface. The findings align well with the study by Obasi et al. (2013) and Yahia et al. (2023) where blends of polypropylene (PP) and plasticized cassava starch (PCS) showed similarities in enzymatic degradation and biodegradability in the blends. The comprehensive study concluded that all developed blended films exhibited rapid biodegradability within 21 days, highlighting their potential as a practical solution to combat improper disposal of such materials in the environment (La Fuente et al., 2023).

Table 3.18 Weight change (%) of PS-based films in degradation

Time (days)	NPSF	ANNF	HMTF
7	51.64 ± 2.36^{b}	55.26 ± 1.52^{a}	55.11 ± 1.44^{a}
14	96.20 ± 3.31^{a}	97.22 ± 2.69^{a}	97.15 ± 4.56^{a}

Values are reported as mean ± standard deviation of three replications. Means followed by the same superscript small letters within a column are not significantly different ($p>0.05$)

Table 3.19 Weight change (%) of casein-based films in degradation

Time (days)	NCF	ATF 15	ATF 30	UTF 15	UTF 30
7	48.96 ±2.23[a]	45.28± 3.01[b]	43.21± 2.98[c]	48.21±2.77[a]	48.63±2.63[a]
14	93.23 ±3.54[c]	94.25±3.75[b]	93.65±3.98[b]	98.12±4.65[a]	98.98±4.87[a]

NC- Native Casein, US- ultrasound treated casein, AC- Autoclave treated casein. Values are reported as mean ± standard deviation of three replications. Means followed by the same superscript small letters within a column are not significantly different (*p>0.05*)

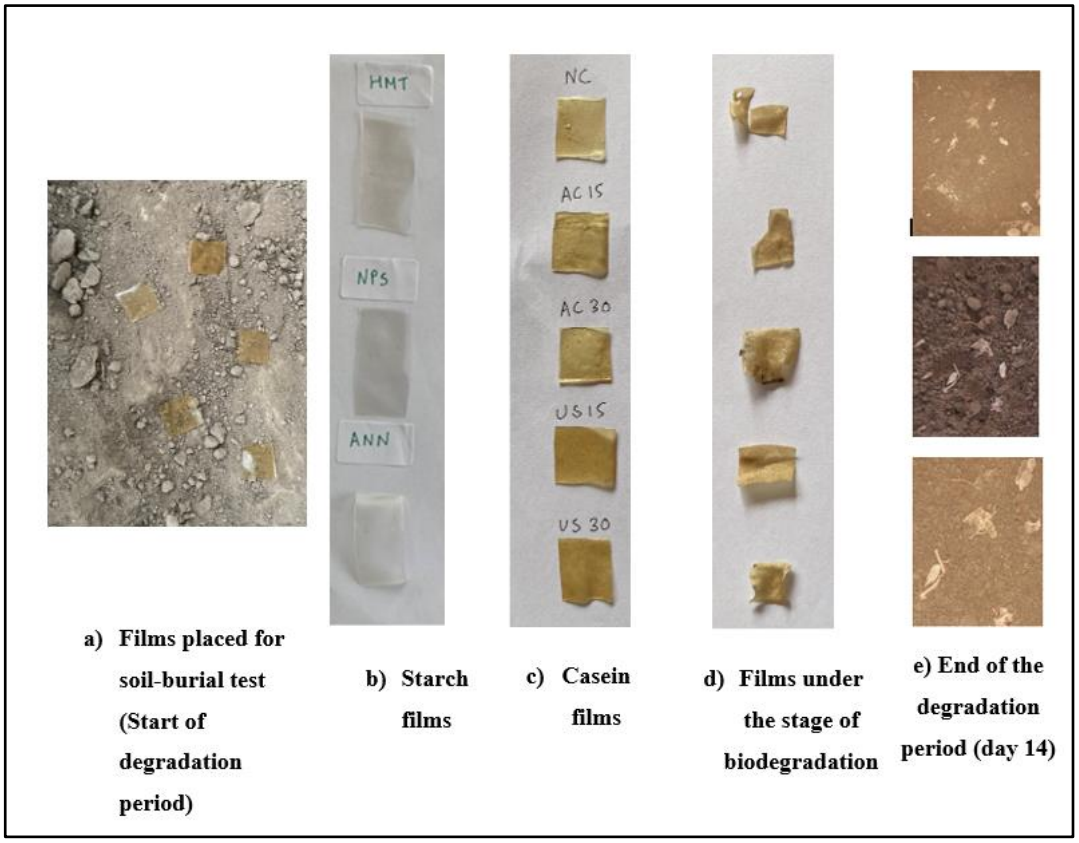

Fig. 3.11 Biodegradability assay images of PS and casein films at various stages of degradation period (till 2 weeks)

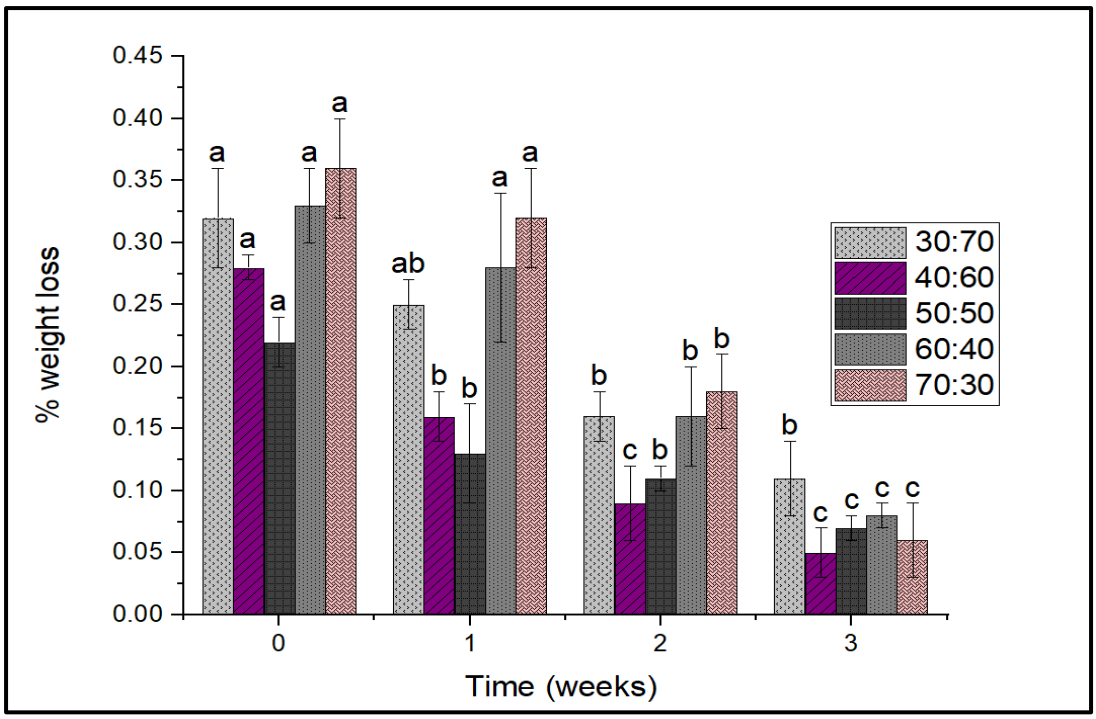

Fig. 3.12 Degradation of PS-casein blended films over 3 weeks. Data presented as different letters on the bar diagram show the significant differences ($p<0.05$).

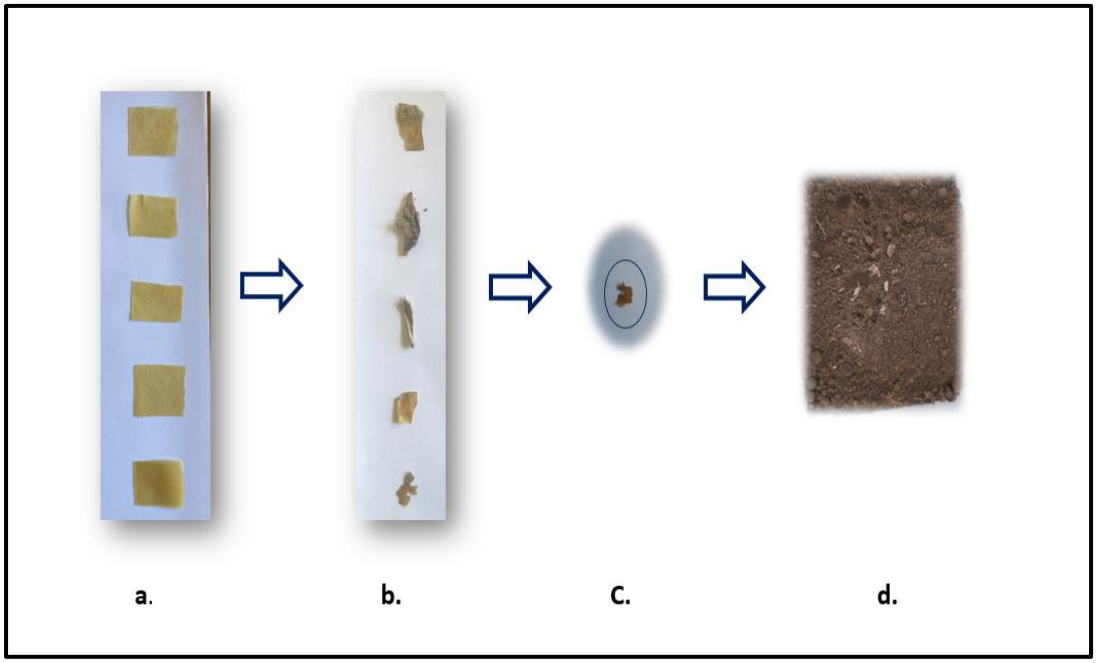

Fig. 3.13 Breakdown of PS-casein blended film within 3 weeks: a) PS-casein blended film (30:70, 40:60, 50:50, 60:40, 70:30) b), and c) Reduction in mass of developed film during soil burial test over successive days d) Absence of any remnants of processed film after 3 weeks.

3.5. Conclusion

The findings of this chapter highlight the significant influence of modified starch on PS-based films, enhancing their mechanical strength, transparency, and solubility. Both annealing and heat-moisture treatments improved tensile strength (TS), elongation at break (EAB%), and reduced solubility and water vapor permeability (WVP). Modified starch films outperformed native ones in mechanical properties, transparency, and solubility. Rheological measurements confirmed their non-Newtonian fluid behavior, while biodegradability tests showed decomposition within 15 days. Films produced from HMTF had superior mechanical strength, lower solubility, better thermal and reduced WVP compared to annealed and native starch films. The ability of modified starches to form better films suggests their potential as biodegradable packaging materials. Additionally, casein films, enhanced by ultrasound (US) and autoclave (AC) treatments, exhibited improved functional properties. US-treated casein films (UTF) showed better mechanical strength, thermally stable and reduced WVP, with 30-min ultrasound treatment yielding the best results. AC-treated casein films also improved mechanical properties but to a lesser extent than ultrasound treatment. Blended PS-casein films (50:50) were clearer, flexible, and displayed a smooth surface with superior mechanical and barrier properties. These films demonstrated reduced light absorption, enhancing UV barrier properties, and biodegraded within 21 days. Thus, PS (HMTF) and casein (UTF 30) in a 50:50 proportion have demonstrated superior physico-chemical, mechanical, thermal, and barrier properties compared to other developed films, making them the focus of further studies in the following chapters. The developed film can however function adeptly as protective wrappers for various items, shielding against environmental factors due to their effective sealing and mechanical characteristics. However, it's worth noting that these films may exhibit sensitivity to moisture, impacting their mechanical properties, and necessitating optimization during processing to achieve desired characteristics across diverse applications.

References to Chapter 3

Abdorreza, M. N., Cheng, L. H., & Karim, A. A., Effects of plasticizers on thermal properties and heat sealability of sago starch films. *Food Hydrocoll.* 2011, *25*(1), 56-60.

Abdullah-Al-Rahim, M. (2021). *A review of wheat gluten-based bioplastics processing and their applications* (Master's thesis, North Dakota State University).

Abedinia, A., Ariffin, F., Huda, N., & Nafchi, A. M. (2018). Preparation and characterization of a novel biocomposite based on duck feet gelatin as alternative to bovine gelatin. *International journal of biological macromolecules*, *109*, 855-862.

Abral, H., Basri, A., Muhammad, F., Fernando, Y., Hafizulhaq, F., Mahardika, M. & Stephane, I. (2019). A simple method for improving the properties of the sago starch films prepared by using ultrasonication treatment. *Food Hydrocolloids*, *93*, 276-283.

Alcázar-Alay, S. C., & Meireles, M. A. A. (2015). Physicochemical properties, modifications and applications of starches from different botanical sources. *Food Science and Technology*, *35*, 215-236.

Aryee, A. N. A., Agyei, D., & Udenigwe, C. C. (2018). Impact of processing on the chemistry and functionality of food proteins. In *Proteins in food processing* (pp. 27-45). Woodhead Publishing.

Arzeni, C., Pérez, O. E., & Pilosof, A. M. (2012). Functionality of egg white proteins as affected by high intensity ultrasound. *Food Hydrocolloids*, *29*(2), 308-316.

Ashogbon, A. O., & Akintayo, E. T. (2014). Recent trend in the physical and chemical modification of starches from different botanical sources: A review. *Starch-Stärke*, *66*(1-2), 41-57.

Asrofi, M., Abral, H., Putra, Y. K., Sapuan, S. M., & Kim, H. J. (2018). Effect of duration of sonication during gelatinization on properties of tapioca starch water hyacinth fiber biocomposite. *International journal of biological macromolecules*, *108*, 167-176.

ASTM, American Society for Testing and Materials, Standard methods for Water vapor Transmission of Materials, E96, Philadelphia, 1995

ASTM, American Society for Testing and Materials, Standard test method for tensile properties of thin plastic sheeting, method D-882-91, Philadelphia, 1995.

ASTM, American Society for Testing and Materials, Standard Test Method for Seal Strength of Flexible Barrier Materials, 15.09 (2009) 6.

ASTM. American Society for Testing and Materials. Standards for measuring plastic film thickness, method 065, 1995 Philadelphia.

Badwaik, L. S., Borah, P. K., & Deka, S. C., Antimicrobial and enzymatic antibrowning film used as coating for bamboo shoot quality improvement. *Carbohydr. Polym.* 2014, *103*, 213-220.

Banerjee, R., Chen, H., & Wu, J. (1996). Milk protein-based edible film mechanical strength changes due to ultrasound process. *Journal of Food Science*, *61*(4), 824-828.

Barać, M., Stanojević, S., Jovanović, S., & Pešić, M. (2004). Soy protein modification: A review. *Acta periodica technologica*, (35), 3-16.

Basiak, E., Lenart, A., & Debeaufort, F., Effect of starch type on the physico-chemical properties of edible films. *Int. J. Biol. Macromol.* 2017, *98*, 348-356.

Basumatary, I. B., Mukherjee, A., Katiyar, V., & Kumar, S. (2022). Biopolymer-based nanocomposite films and coatings: Recent advances in shelf-life improvement of fruits and vegetables. *Critical Reviews in Food Science and Nutrition*, *62*(7), 1912-1935.

Bertoft, E. (2017). Understanding starch structure: Recent progress. *Agronomy*, *7*(3), 56.

Bhat, M. Y., Dar, T. A., & Singh, L. R. (2016). Casein proteins: structural and functional aspects. *Milk proteins-From structure to biological properties and health aspects*, *10*, 64187.

Biduski, B., da Silva, F. T., da Silva, W. M., El Halal, S. L. D. M., Pinto, V. Z., Dias, A. R. G., & da Rosa Zavareze, E. (2017). Impact of acid and oxidative modifications, single or dual, of sorghum starch on biodegradable films. *Food Chemistry*, *214*, 53-60.

Biswas, B., & Sit, N. (2020). Effect of ultrasonication on functional properties of tamarind seed protein isolates. *Journal of food science and technology*, *57*(6), 2070-2078.

Borah, P. P., Das, P., & Badwaik, L. S. (2017). Ultrasound treated potato peel and sweet lime pomace-based biopolymer film development. *Ultrasonics sonochemistry*, *36*, 11-19.

Brahma, B., & Sit, N. (2020). Physicochemical properties and digestibility of heat moisture–treated potato starches for different treatment conditions. *Potato Research*, *63*, 367-383.

Bußler, S., Steins, V., Ehlbeck, J., & Schlüter, O. (2015). Impact of thermal treatment versus cold atmospheric plasma processing on the techno-functional protein properties from Pisum sativum 'Salamanca'. *Journal of Food Engineering*, *167*, 166-174.

Butt, M. S., & Rizwana, B. (2010). Nutritional and functional properties of some promising legumes protein isolates. *Pakistan Journal of Nutrition*, *9*(4), 373-379.

Cai, L., Shi, Y. C., Rong, L., & Hsiao, B. S. (2010). Debranching and crystallization of waxy maize starch in relation to enzyme digestibility. *Carbohydrate Polymers*, *81*(2), 385-393.

Calva-Estrada, S. J., Jiménez-Fernández, M., & Lugo-Cervantes, E., Protein-based films: Advances in the development of biomaterials applicable to food packaging. *Food Engg. Rev.* 2019, *11*(2), 78-92.

Camire, M. E., Kubow, S., & Donnelly, D. J., Potatoes and human health. *Critical reviews in food science and nutrition* 2009, *49*(10), 823-840.

Çelik, H. Yaman, S. Turan, A. Kara, F. Kara, B. Zhu, B., D.A. Dutta, J. Mater. Process. Technol. 1 (1) (2018) 1–8.

Chambi, H., & Grosso, C. (2006). Edible films produced with gelatin and casein cross-linked with transglutaminase. *Food research international*, *39*(4), 458-466.

Chambi, H., & Grosso, C. (2006). Edible films produced with gelatin and casein cross-linked with transglutaminase. *Food research international*, *39*(4), 458-466.

Chandrapala, J., Zisu, B., Palmer, M., Kentish, S., & Ashokkumar, M. (2011). Effects of ultrasound on the thermal and structural characteristics of proteins in reconstituted whey protein concentrate. *Ultrasonics sonochemistry*, *18*(5), 951-957.

Chassenieux, C., & Jyotishkumar, P. Biopolymer-Based Materials. *Networks*, *80*, 849.

Chemat, F., & Khan, M. K. (2011). Applications of ultrasound in food technology: processing, preservation and extraction. *Ultrasonics sonochemistry*, *18*(4), 813-835.

Choi, I., Chun, J., Choi, H.S., Park, J., Kim, N.G., Lee, S.K., Park, C.H., Jeong, K.H., Nam, J.W., Cho, J. and Cho, K., Starch characteristics, sugars and thermal properties of processing potato (Solanum tuberosum L.) cultivars developed in Korea. *Am. J. Potato Res*. 2020., *97*(3), 308-317.

Chollakup, R., Pongburoos, S., Boonsong, W., Khanoonkon, N., Kongsin, K., Sothornvit, R., & Harnkarnsujarit, N. (2020). Antioxidant and antibacterial activities of cassava starch and whey protein blend films containing rambutan peel extract and cinnamon oil for active packaging. *Lwt*, *130*, 109573.

Chung, H. J., Liu, Q., & Hoover, R. (2009). Impact of annealing and heat-moisture treatment on rapidly digestible, slowly digestible and resistant starch levels in native and gelatinized corn, pea and lentil starches. *Carbohydrate polymers*, *75*(3), 436-447.

Colla, E., do Amaral Sobral, P. J., & Menegalli, F. C., Amaranthus cruentus flour edible films: influence of stearic acid addition, plasticizer concentration, and emulsion stirring speed on water vapor permeability and mechanical properties. *J. Agric. Food Chem.* 2006, *54*(18), 6645-6653.

Cortés-Rodríguez, M., Villegas-Yépez, C., González, J. H. G., Rodríguez, P. E., & Ortega-Toro, R. (2020). Development and evaluation of edible films based on cassava starch, whey protein, and bees wax. *Heliyon*, *6*(9), e04884.

Cruz-Diaz, K., Cobos, Á., Fernández-Valle, M. E., Díaz, O., & Cambero, M. I. (2019). Characterization of edible films from whey proteins treated with heat, ultrasounds and/or transglutaminase. Application in cheese slices packaging. *Food Packaging and Shelf Life*, *22*, 100397.

da Rosa Zavareze, E., Pinto, V. Z., Klein, B., El Halal, S. L. M., Elias, M. C., Prentice-Hernández, C., & Dias, A. R. G., Development of oxidized and heat–moisture treated potato starch film. *Food Chem.* 2012, *132*(1), 344-350.

Das, M., & Chowdhury, T. (2016). Heat sealing property of starch based self-supporting edible films. *Food Packaging and Shelf Life*, *9*, 64-68.

de Azevedo, L.C., Rovani, S., Santos, J.J., Dias, D.B., Nascimento, S.S., Oliveira, F.F., Silva, L.G. & Fungaro, D.A., Biodegradable films derived from corn and potato starch and study of the effect of silicate extracted from sugarcane waste ash. *ACS Appl. Polym. Mat.* 2020, *2*(6), pp.2160-2169.

De Maria, S., Ferrari, G., & Maresca, P. (2016). Effects of high hydrostatic pressure on the conformational structure and the functional properties of bovine serum albumin. *Innovative Food Science & Emerging Technologies*, *33*, 67-75.

de Moraes Crizel, T., de Oliveira Rios, A., D Alves, V., Bandarra, N., Moldão-Martins, M., & Hickmann Flôres, S., Biodegradable films based on gelatin and papaya peel microparticles with antioxidant properties. *Food Bioproc. Technol.* 2018, *11*(3), 536-550.

Deka, D., & Sit, N. (2016). Dual modification of taro starch by microwave and other heat moisture treatments. *International Journal of Biological Macromolecules*, *92*, 416-422.

Deng, C. (2023). Technology of physically modification of potato starch and their applications in food products.

Devi, R., & Sit, N. (2019). Effect of single and dual steps annealing in combination with hydroxypropylation on physicochemical, functional and rheological properties of barley starch. *International journal of biological macromolecules*, *129*, 1006-1014.

Dey, A., & Sit, N. (2017). Modification of foxtail millet starch by combining physical, chemical and enzymatic methods. *International journal of biological macromolecules*, *95*, 314-320.

Farris, S., Schaich, K. M., Liu, L., Piergiovanni, L., & Yam, K. L. (2009). Development of polyion-complex hydrogels as an alternative approach for the production of bio-based

polymers for food packaging applications: a review. *Trends in food science & technology*, *20*(8), 316-332.

Flores-Jiménez, N. T., Ulloa, J. A., Silvas, J. E. U., Ramírez, J. C. R., Ulloa, P. R., Rosales, P. U. B., & Leyva, R. G. (2019). Effect of high-intensity ultrasound on the compositional, physicochemical, biochemical, functional and structural properties of canola (Brassica napus L.) protein isolate. *Food Research International*, *121*, 947-956.

Fonseca, L. M., El Halal, S. L. M., Dias, A. R. G., & da Rosa Zavareze, E. (2021). Physical modification of starch by heat-moisture treatment and annealing and their applications: A review. *Carbohydrate Polymers*, *274*, 118665.

Fonseca, L. M., Henkes, A. K., Bruni, G. P., Viana, L. A. N., de Moura, C. M., Flores, W. H., & Galio, A. F. (2018). Fabrication and characterization of native and oxidized potato starch biodegradable films. *Food Biophysics*, *13*, 163-174.

Fredi, G., & Dorigato, A. (2023). Compatibilization of biopolymer blends: a review. *Advanced Industrial and Engineering Polymer Research*.

Galus, S., & Kadzińska, J. (2015). Food applications of emulsion-based edible films and coatings. *Trends in Food Science & Technology*, *45*(2), 273-283.

Galus, S., & Kadzińska, J. (2016). Whey protein edible films modified with almond and walnut oils. *Food Hydrocolloids*, *52*, 78-86.

García-Guzmán, L., Cabrera-Barjas, G., Soria-Hernández, C. G., Castaño, J., Guadarrama-Lezama, A. Y., & Rodríguez Llamazares, S. (2022). Progress in starch-based materials for food packaging applications. *Polysaccharides*, *3*(1), 136-177.

Gomes, A. M., da Silva, C. E. M., & Ricardo, N. M. (2005). Effects of annealing on the physicochemical properties of fermented cassava starch (polvilho azedo). *Carbohydrate Polymers*, *60*(1), 1-6.

Guzman-Puyol, S., Benítez, J. J., & Heredia-Guerrero, J. A. (2022). Transparency of polymeric food packaging materials. *Food Research International*, *161*, 111792.

Han, T., Wang, M., Wang, Y., & Tang, L. (2020). Effects of high-pressure homogenization and ultrasonic treatment on the structure and characteristics of casein. *LWT*, *130*, 109560.

Hassan, B., Chatha, S. A. S., Hussain, A. I., Zia, K. M., & Akhtar, N. (2018). Recent advances on polysaccharides, lipids and protein based edible films and coatings: A review. *International journal of biological macromolecules*, *109*, 1095-1107.

Hirpara, N. J., Dabhi, M. N., & Rathod, P. J. (2021). Development of potato starch based biodegradable packaging film. *J. Food Process. Technol*, *12*, 529-541.

Hoque, M. E., Ye, T. J., Yong, L. C., & Dahlan, K. M., Sago starch-mixed low-density polyethylene biodegradable polymer: synthesis and characterization. J. Mater. *2013*, 2013, 1-7.

Hormdok, R., & Noomhorm, A. (2007). Hydrothermal treatments of rice starch for improvement of rice noodle quality. *LWT-Food science and Technology*, *40*(10), 1723-1731.

Hu, A., Wang, X., Li, L., Xu, T., & Zheng, J. (2020). Effects of annealing time on structure and properties of sweet potato starch. *Cereal Chemistry*, *97*(3), 573-580.

Huntrakul, K., Yoksan, R., Sane, A., & Harnkarnsujarit, N. (2020). Effects of pea protein on properties of cassava starch edible films produced by blown-film extrusion for oil packaging. *Food Packaging and shelf life*, *24*, 100480.

Iuga, M., & Mironeasa, S. (2020). A review of the hydrothermal treatments impact on starch based systems properties. *Critical Reviews in Food Science and Nutrition*, *60*(22), 3890-3915.

Izzi, Y. S., Gerschenson, L. N., Jagus, R. J., & Ollé Resa, C. P. (2023). Edible Films Based on Tapioca Starch and WPC or Gelatine Plasticized with Glycerol: Potential Food Applications Based on Their Mechanical and Heat-Sealing Properties. *Food and Bioprocess Technology*, 1-11.

Jacobs, H., & Delcour, J. A. (1998). Hydrothermal modifications of granular starch, with retention of the granular structure: A review. *Journal of agricultural and food chemistry*, *46*(8), 2895-2905.

Jagadeesan, S., Govindaraju, I., & Mazumder, N. (2020). An insight into the ultrastructural and physiochemical characterization of potato starch: a review. *American Journal of Potato Research*, *97*(5), 464-476.

Jain, N., Singh, V. K., & Chauhan, S. (2018). Dynamic and creep analysis of polyvinyl alcohol based films blended with starch and protein. *Journal of Polymer Engineering*, *39*(1), 35-47.

Jambrak, A. R., Lelas, V., Mason, T. J., Krešić, G., & Badanjak, M. (2009). Physical properties of ultrasound treated soy proteins. *Journal of Food Engineering*, *93*(4), 386-393.

Jambrak, A. R., Mason, T. J., Lelas, V., Herceg, Z., & Herceg, I. L. (2008). Effect of ultrasound treatment on solubility and foaming properties of whey protein suspensions. *Journal of food engineering*, *86*(2), 281-287.

Jiang, L., Wang, J., Li, Y., Wang, Z., Liang, J., Wang, R., & Zhang, M. (2014). Effects of ultrasound on the structure and physical properties of black bean protein isolates. *Food Research International*, *62*, 595-601.

Jiang, T., Duan, Q., Zhu, J., Liu, H., & Yu, L. (2020). Starch-based biodegradable materials: Challenges and opportunities. *Advanced Industrial and Engineering Polymer Research*, *3*(1), 8-18.

Jiang, Z. Q., Pulkkinen, M., Wang, Y. J., Lampi, A. M., Stoddard, F. L., Salovaara, H., & Sontag-Strohm, T. (2016). Faba bean flavour and technological property improvement by thermal pre-treatments. *LWT-Food Science and Technology*, *68*, 295-305.

Jooyandeh, H. (2011). Whey protein films and coatings: A review. *Pakistan Journal of Nutrition*, *10*(3), 296-301.

Kandasamy, S., Yoo, J., Yun, J., Kang, H. B., Seol, K. H., Kim, H. W., & Ham, J. S.

(2021). Application of whey protein-based edible films and coatings in food industries: An updated overview. *Coatings*, *11*(9), 1056.

Kaur, B., Ariffin, F., Bhat, R., & Karim, A. A. (2012). Progress in starch modification in the last decade. *Food hydrocolloids*, *26*(2), 398-404.

Khan, S. H., Butt, M. S., Sharif, M. K., Sameen, A., Mumtaz, S., & Sultan, M. T. (2011). Functional properties of protein isolates extracted from stabilized rice bran by microwave, dry heat, and parboiling. *Journal of Agricultural and Food Chemistry*, *59*(6), 2416-2420.

Khoshkalampour, A., Ahmadi, S., Ghasempour, Z., Lim, L. T., & Ghorbani, M. (2023). Development of a novel film based on casein/modified tragacanth gum enriched by carbon quantum dots for shelf-life extension of butter. *Food and Bioprocess Technology*, 1-18.

Khwaldia, K., Perez, C., Banon, S., Desobry, S., & Hardy, J. (2004). Milk proteins for edible films and coatings. *Critical Reviews in Food Science and Nutrition*, *44*(4), 239-251.Krešić, G., Lelas, V.

Kocira, Anna, Katarzyna Kozłowicz, Katarzyna Panasiewicz, Mariola Staniak, Ewa Szpunar-Krok, and Paulina Hortyńska. "Polysaccharides as edible films and coatings: Characteristics and influence on fruit and vegetable quality—A review." *Agronomy* 11, no. 5 (2021): 813.

Kumar, A., Mishra, R. K., Verma, K., Aldosari, S. M., Maity, C. K., Verma, S., & Thakur, V. K. (2023). A Comprehensive Review of Various Biopolymer Composites and Their Applications: From Biocompatibility To Self-Healing. *Materials Today Sustainability*, 100431.

Kumar, R., Ghoshal, G., & Goyal, M. (2021). Biodegradable composite films/coatings of modified corn starch/gelatin for shelf life improvement of cucumber. *Journal of Food Science and Technology*, *58*, 1227-1237.

La Fuente, C. I., Atanazio-Silva, G. A., Anjos, C. A., & Tadini, C. C. (2023). Biodegradability of bio-based materials produced with dry heating treatment-modified cassava starch. *Journal of Applied Polymer Science*, *140*(46), e54679.

Lee, H. L., & Yoo, B. (2011). Effect of hydroxypropylation on physical and rheological properties of sweet potato starch. *LWT-Food Science and Technology*, *44*(3), 765-770.

Lee, Y. Y., Yusof, Y. A., & Pui, L. P. (2020). Development of milk protein edible films incorporated with Lactobacillus rhamnosus GG. *BioResources*, *15*(3), 6960-6973.

Li, H., Wang, J., Liu, Y., Chen, J., Wang, C., Hu, Y., & Hu, K. (2024). Production of biodegradable potato starch films containing Lycium barbarum polysaccharide and investigation of their physicochemical properties. *Food Packaging and Shelf Life*, *44*, 101320.

Li, H., Zhai, F., Li, J., Zhu, X., Guo, Y., Zhao, B., & Xu, B. (2021). Physicochemical properties and structure of modified potato starch granules and their complex with tea polyphenols. *International Journal of Biological Macromolecules*, *166*, 521-528.

Li, M. N., Zhang, B., Xie, Y., & Chen, H. Q. (2019). Effects of debranching and repeated heat-moisture treatments on structure, physicochemical properties and in vitro digestibility of wheat starch. *Food Chemistry*, *294*, 440-447.

Li, Q., Zheng, J., Ge, G., Zhao, M., & Sun, W. (2020). Impact of heating treatments on physical stability and lipid-protein co-oxidation in oil-in-water emulsion prepared with soy protein isolates. *Food Hydrocolloids*, *100*, 105167.

Lin, Z., Xia, Y., Yang, G., Chen, J., & Ji, D. (2019). Improved film formability of oxidized starch-based blends through controlled modification with cellulose nanocrystals. *Industrial crops and products*, *140*, 111665.

Liu, C., Huang, J., Zheng, X., Liu, S., Lu, K., Tang, K., & Liu, J. (2020). Heat sealable soluble soybean polysaccharide/gelatin blend edible films for food packaging applications. *Food Packaging and Shelf Life*, *24*, 100485.

Liu, C., Yu, B., Tao, H., Liu, P., Zhao, H., Tan, C., & Cui, B. (2021). Effects of soy protein isolate on mechanical and hydrophobic properties of oxidized corn starch film. *Lwt*, *147*, 111529.

Liu, D., Zhao, P., Chen, J., Yan, Y., & Wu, Z. (2022). Recent advances and applications

in starch for intelligent active food packaging: A review. *Foods*, *11*(18), 2879.

Liu, H., Lv, M., Wang, L., Li, Y., Fan, H., & Wang, M. (2016). Comparative study: How annealing and heat-moisture treatment affect the digestibility, textural, and physicochemical properties of maize starch. *Starch-Stärke*, *68*(11-12), 1158-1168.

Lourdin, D., Della Valle, G., & Colonna, P., Influence of amylose content on starch films and foams. *Carbohydr. Polym.* 1995, *27*(4), 261-270.

Luchese, C. L., Frick, J. M., Patzer, V. L., Spada, J. C., & Tessaro, I. C., Synthesis and characterization of biofilms using native and modified pinhão starch. *Food Hydrocoll.* 2015, *45*, 203-210.

Mali, S., Grossmann, M. V. E., García, M. A., Martino, M. N., & Zaritzky, N. E. (2005). Mechanical and thermal properties of yam starch films. *Food Hydrocolloids*, *19*(1), 157-164.

Manchun, S., Nunthanid, J., Limmatvapirat, S., & Sriamornsak, P. (2012). Effect of ultrasonic treatment on physical properties of tapioca starch. *Advanced materials research*, *506*, 294-297.

Marboh, V., & Mahanta, C. L., Physicochemical and rheological properties and in vitro digestibility of heat moisture treated and annealed starch of sohphlang (Flemingia vestita) tuber. *Int. J. Biol. Macromol.* 2021, *168*, 486-495.

Meng, Y., Liang, Z., Zhang, C., Hao, S., Han, H., Du, P., & Liu, L. (2021). Ultrasonic modification of whey protein isolate: Implications for the structural and functional properties. *Lwt*, *152*, 112272.

Menzel, C. (2014). *Starch structures and their usefulness in the production of packaging materials* (No. 2014: 90).

Mi, T., Zhang, X., Liu, P., Gao, W., Li, J., Xu, N., & Cui, B. (2023). Ultrasonication effects on physicochemical properties of biopolymer-based films: A comprehensive review. *Critical Reviews in Food Science and Nutrition*, *63*(21), 5044-5062.

Mi, T., Zhang, X., Liu, P., Gao, W., Li, J., Xu, N., & Cui, B. (2021). Ultrasonication effects

on physicochemical properties of biopolymer-based films: A comprehensive review. *Critical Reviews in Food Science and Nutrition*, 1-19.

Mihalca, V., Kerezsi, A. D., Weber, A., Gruber-Traub, C., Schmucker, J., Vodnar, D. C., & Pop, O. L. (2021). Protein-based films and coatings for food industry applications. *Polymers*, *13*(5), 769.

Mishra, A., Mann, B., Poonia, A., Rai, D. C., & Hooda, A. (2022). Milk Protein-Based Edible Coatings: Properties and Applications. In *Edible Food Packaging: Applications, Innovations and Sustainability* (pp. 217-232). Singapore: Springer Nature Singapore.

Mittal, A., Garg, S., Premi, A., & Giri, A. S. (2021). Synthesis of polyvinyl alcohol/modified starch-based biodegradable nanocomposite films reinforced with starch nanocrystals for packaging applications. *Polymers and Polymer Composites*, *29*(5), 405-416.

Monroy, Y., Rivero, S., & García, M. A. (2018). Microstructural and techno-functional properties of cassava starch modified by ultrasound. *Ultrasonics sonochemistry*, *42*, 795-804.

Moon, B. (2002). *The effect of preheating on solubility and emulsion stability of whey protein concentrates*. The Ohio State University.

More, P. R., Pegu, K., & Arya, S. S. (2022). Development and characterization of taro starch-casein composite bioactive films functionalized by micellar pomegranate peel extract (MPPE). *International Journal of Biological Macromolecules*, *220*, 1060-1071.

Niranjana Prabhu, T., & Prashantha, K. (2018). A review on present status and future challenges of starch-based polymer films and their composites in food packaging applications. *Polymer Composites*, *39*(7), 2499-2522.

Niu, X., Ma, Q., Li, S., Wang, W., Ma, Y., Zhao, H., ... & Wang, J. (2021). Preparation and characterization of biodegradable composited films based on potato starch/glycerol/gelatin. *Journal of Food Quality*, *2021*(1), 6633711.

Obasi, H. C., Igwe, I. O., & Madufor, I. C. (2013). Effect of soil burial on tensile properties

of polypropylene/plasticized cassava starch blends. *Advances in Materials Science and Engineering*, *2013*(1), 326538.

Ogechukwu, C. O., and Ikechukwu, J. O. (2017). Effect of heat processing treatments on the chemical composition and functional properties of lima bean (Phaseolus lunatus) flour. *American Journal of Food Sciences and Nutrition*, *1*(1), 14-24.

Osés, J., Fabregat-Vázquez, M., Pedroza-Islas, R., Tomás, S. A., Cruz-Orea, A., & Maté, J. I. (2009). Development and characterization of composite edible films based on whey protein isolate and mesquite gum. *Journal of Food Engineering*, *92*(1), 56-62.

P. Taylor, J. Jane, Part A : Pure and Applied Chemistry Starch Properties , Modifications and Applications, *J. Macromol. Sci. A*. 2013, 37–41.

Pranoto, Y., & Rakshit, S. K. (2014). Physicochemical properties of heat moisture treated sweet potato starches of selected Indonesian varieties. *International Food Research Journal*, *21*(5), 2031.

Pratiwi, M., Faridah, D. N., & Lioe, H. N. (2018). Structural changes to starch after acid hydrolysis, debranching, autoclaving-cooling cycles, and heat moisture treatment (HMT): A review. *Starch-Stärke*, *70*(1-2), 1700028.

Qamar, S., Bhandari, B., & Prakash, S. (2019). Effect of different homogenisation methods and UHT processing on the stability of pea protein emulsion. *Food research international*, *116*, 1374-1385.

Raigond, P., Sood, A., Kalia, A., Joshi, A., Kaundal, B., Raigond, B., ... & Chakrabarti, S. K. (2019). Antimicrobial activity of potato starch-based active biodegradable nanocomposite films. *Potato Research*, *62*, 69-83.

Ramos, Ó. L., Reinas, I., Silva, S. I., Fernandes, J. C., Cerqueira, M. A., Pereira, R. N., & Malcata, F. X. (2013). Effect of whey protein purity and glycerol content upon physical properties of edible films manufactured therefrom. *Food Hydrocolloids*, *30*(1), 110-122.

Rico, D., Villaverde, A., Martinez-Villaluenga, C., Gutierrez, A. L., Caballero, P. A., Ronda, F., & Martin Diana, A. B. (2020). Application of autoclave treatment for

development of a natural wheat bran antioxidant ingredient. *Foods*, *9*(6), 781.

Rizwana, S., & Hazarika, M. K. (2022). Near infrared-based process analytical technology module for estimating gelatinization optimal point. *Journal of Food Process Engineering*, *45*(3), e13987.

Roy, S., Malik, B., Chawla, R., Bora, S., Ghosh, T., Santhosh, R., & Sarkar, P. (2024). Biocompatible film based on protein/polysaccharides combination for food packaging applications: A comprehensive review. *International Journal of Biological Macromolecules*, 134658.

Said, N. S., Howell, N. K., & Sarbon, N. M. (2023). A review on potential use of gelatin-based film as active and smart biodegradable films for food packaging application. *Food Reviews International*, *39*(2), 1063-1085.

Sarv, V., Trass, O., & Diosady, L. L. (2017). Preparation and characterization of Camelina sativa protein isolates and mucilage. *Journal of the American Oil Chemists' Society*, *94*(10), 1279-1285.

Schafranski, K., Ito, V. C., & Lacerda, L. G. (2021). Impacts and potential applications: A review of the modification of starches by heat-moisture treatment (HMT). *Food Hydrocolloids*, *117*, 106690.

Seifdavati, J., & Taghizadeh, A. (2012). Effects of moist heat treatment on ruminal nutrient degradability of and in vitro intestinal digestibility of crude protein from some of legume seeds. *J. Food Agric. Env*, *10*, 390-397.

Shanthilal, J., & Bhattacharya, S. (2015). Rheology of rice flour dough with gum arabic: small and large-deformation studies, sensory assessment and modeling. *Journal of food science*, *80*(8), E1735-E1745.

Shen, X., Shao, S., & Guo, M. (2017). Ultrasound-induced changes in physical and functional properties of whey proteins. *International Journal of Food Science & Technology*, *52*(2), 381-388.

Shi, A. M., Wang, L. J., Li, D., & Adhikari, B. (2013). Characterization of starch films containing starch nanoparticles: Part 1: Physical and mechanical properties. *Carbohydrate Polymers*, *96*(2), 593-601.

Shojaei, M., Eshaghi, M., & Nateghi, L. (2019). Characterization of hydroxypropyl methyl cellulose–whey protein concentrate bionanocomposite films reinforced by chitosan nanoparticles. *Journal of food processing and preservation*, *43*(10), e14158.

Silva, N. H., Vilela, C., Almeida, A., Marrucho, I. M., & Freire, C. S. (2018). Pullulan-based nanocomposite films for functional food packaging: Exploiting lysozyme nanofibers as antibacterial and antioxidant reinforcing additives. *Food Hydrocolloids*, *77*, 921-930.

Singh, G. D., Bawa, A. S., Riar, C. S., & Saxena, D. C., Influence of heat-moisture treatment and acid modifications on physicochemical, rheological, thermal and morphological characteristics of Indian water chestnut (Trapa natans) starch and its application in biodegradable films. *Starch-Stärke.* 2009, *61*(9), 503-513.

Singh, N., Isono, N., Srichuwong, S., Noda, T., & Nishinari, K. (2008). Structural, thermal and viscoelastic properties of potato starches. *Food Hydrocolloids*, *22*(6), 979-988.

Singh, S., & Kaur, M., Steady and dynamic shear rheology of starches from different oat cultivars in relation to their physicochemical and structural properties. *Int. J. Food Prop.* 2017, *20*(12), 3282-3294.

Singh, S., Raina, C. S., Bawa, A. S., & Saxena, D. C. (2005). Effect of heat-moisture treatment and acid modification on rheological, textural, and differential scanning calorimetry characteristics of sweetpotato starch. *Journal of Food Science*, *70*(6), e373-e378.

Sit, N., Misra, S., & Deka, S. C. (2013). Physicochemical, functional, textural and colour characteristics of starches isolated from four taro cultivars of North-E ast India. *Starch-Stärke*, *65*(11-12), 1011-1021.

Stute, R., Hydrothermal modification of starches: The difference between annealing and heat/moisture-treatment. *Starch-Stärke* 1992, *44*(6), 205-214.

Su, C. Y., Li, D., Wang, L. J., & Wang, Y. (2023). Biodegradation behavior and digestive properties of starch-based film for food packaging–a review. *Critical Reviews in Food Science and Nutrition*, *63*(24), 6923-6945.

Subroto, E., Indiarto, R., Marta, H., & Shalihah, S. (2019). Effect of heat-moisture treatment on functional and pasting properties of potato (Solanum tuberosum L. var. Granola) starch. *Food Research*, (5), 469-476.

Sukhija, S., Singh, S., & Riar, C. S. (2016). Analyzing the effect of whey protein concentrate and psyllium husk on various characteristics of biodegradable film from lotus (Nelumbo nucifera) rhizome starch. *Food Hydrocolloids*, *60*, 128-137.

Sukhija, S., Singh, S., & Riar, C. S. (2019). Development and characterization of biodegradable films from whey protein concentrate, psyllium husk and oxidized, crosslinked, dual-modified lotus rhizome starch composite. *Journal of the Science of Food and Agriculture*, *99*(7), 3398-3409.

Sun, Q., Sun, C., & Xiong, L. (2013). Mechanical, barrier and morphological properties of pea starch and peanut protein isolate blend films. *Carbohydrate polymers*, *98*(1), 630-637.

Tako, M., & Hizukuri, S., Gelatinization mechanism of potato starch. *Carbohydr. Polym.* 2002, *48*(4), 397-401.

Tian, R., Feng, J., Huang, G., Tian, B., Zhang, Y., Jiang, L., & Sui, X. (2020). Ultrasound driven conformational and physicochemical changes of soy protein hydrolysates. *Ultrasonics sonochemistry*, *68*, 105202.

Tomasula, P. M., Craig Jr, J. C., Boswell, R. T., Cook, R. D., Kurantz, M. J., & Maxwell, M. (1995). Preparation of casein using carbon dioxide. *Journal of dairy science*, *78*(3), 506-514.

Trung, P. T. B., Ngoc, L. B. B., Hoa, P. N., Tien, N. N. T., & Van Hung, P. (2017). Impact of heat-moisture and annealing treatments on physicochemical properties and digestibility of starches from different colored sweet potato varieties. *International Journal of Biological Macromolecules*, *105*, 1071-1078.

Varatharajan, V., Hoover, R., Liu, Q., & Seetharaman, K. (2010). The impact of heat-moisture treatment on the molecular structure and physicochemical properties of normal and waxy potato starches. *Carbohydrate Polymers*, *81*(2), 466-475.

Wang, C., & Guo, M. (2019). Whey protein structure and denaturation and interactions with other food components. *Whey protein production, chemistry, functionality, and applications*, 67-101.

Wang, C., & Johnson, L. A. (2001). Functional properties of hydrothermally cooked soy protein products. *Journal of the American Oil Chemists' Society*, *78*(2), 189-195.

Wang, K., Wang, W., Ye, R., Liu, A., Xiao, J., Liu, Y., & Zhao, Y. (2017). Mechanical properties and solubility in water of corn starch-collagen composite films: Effect of starch type and concentrations. *Food chemistry*, *216*, 209-216.

Wang, Q., Li, L., & Zheng, X. (2021). Recent advances in heat-moisture modified cereal starch: Structure, functionality and its applications in starchy food systems. *Food Chemistry*, *344*, 128700.

Watcharatewinkul, Y., Puttanlek, C., Rungsardthong, V., & Uttapap, D. (2009). Pasting properties of a heat-moisture treated canna starch in relation to its structural characteristics. *Carbohydrate Polymers*, *75*(3), 505-511.

Wawro, D., & Kazimierczak, J., Forming conditions and mechanical properties of potato starch films. *Fibres & Textiles in Eastern Europe.* 2008, *16*(6), 71.

Whistler, R. L., BeMiller, J. N., & Paschall, E. F. (Eds.). (2012). *Starch: chemistry and technology*. Academic Press.

Wittaya, T. (2012). Protein-based edible films: Characteristics and improvement of properties. *Structure and function of food engineering*, *3*, 44-70.

Woggum, T., Sirivongpaisal, P., & Wittaya, T. (2014). Properties and characteristics of dual-modified rice starch based biodegradable films. *International journal of biological macromolecules*, *67*, 490-502.

Wu, Q., Zhang, X., Jia, J., Kuang, C., & Yang, H. (2018). Effect of ultrasonic pretreatment on whey protein hydrolysis by alcalase: Thermodynamic parameters, physicochemical properties and bioactivities. *Process Biochemistry*, *67*, 46-54.

Wu, W., Hettiarachchy, N. S., Kalapathy, U., & Williams, W. P. (1999). Functional properties and nutritional quality of alkali-and heat-treated soy protein isolate. *Journal of food quality*, *22*(2), 119-133.

Xie, S. X., Liu, Q., & Cui, S. W. (2005). Starch modification and applications. *Food carbohydrates: Chemistry, physical properties, and applications*, 357-405.

Xu, M., Saleh, A. S., Gong, B., Li, B., Jing, L., Gou, M., ... & Li, W. (2018). The effect of repeated versus continuous annealing on structural, physicochemical, and digestive properties of potato starch. *Food Research International*, *111*, 324-333.

Yahia, R., Owda, M. E., Abou-Zeid, R. E., Abdelhai, F., El-Gamil, H. Y., Abdo, A. M., & Ali, A. A. (2023). Biodegradable, UV absorber and thermal stable bioplastic films from waxy corn starch/polyvinyl alcohol blends. *Biomass Conversion and Biorefinery*, 1-18.

Yang, C., Zhong, F., Goff, H. D., & Li, Y. (2019). Study on starch-protein interactions and their effects on physicochemical and digestible properties of the blends. *Food chemistry*, *280*, 51-58.

Yanjun, S., Jianhang, C., Shuwen, Z., Hongjuan, L., Jing, L., Lu, L., & Jiaping, L. (2014). Effect of power ultrasound pre-treatment on the physical and functional properties of reconstituted milk protein concentrate. *Journal of Food Engineering*, *124*, 11-18.

Yashini, M., Khushbu, S., Madhurima, N., Sunil, C. K., Mahendran, R., & Venkatachalapathy, N. (2024). Thermal properties of different types of starch: A review. *Critical Reviews in Food Science and Nutrition*, *64*(13), 4373-4396.

Zhang, R., Wang, X., & Cheng, M., Preparation and characterization of potato starch film with various size of nano-SiO2. *Polymers.* 2018, *10*(10), 1172.

Zhang, R., Wang, Y., Ma, D., Ahmed, S., Qin, W., & Liu, Y. (2019). Effects of ultrasonication duration and graphene oxide and nano-zinc oxide contents on the properties of polyvinyl alcohol nanocomposites. *Ultrasonics sonochemistry*, *59*, 104731.

Zhao, Y., Chen, F., Gao, C., Feng, X., & Tang, X. (2022). Structure, physical and antioxidant properties of quinoa protein/hsian-tsao gum composite biodegradable active films. *Lwt*, *155*, 112985.

Zhuang, Y., Wang, Y., & Yang, H. (2023). Characterizing digestibility of potato starch with cations by SEM, X-ray, LF-NMR, FTIR. *Food Chemistry*, *424*, 136396.

Zink, J., Wyrobnik, T., Prinz, T., & Schmid, M. (2016). Physical, chemical and biochemical modifications of protein-based films and coatings: An extensive review. *International Journal of Molecular Sciences*, *17*(9), 1376.

Zou, J., Xu, M., Tang, W., Wen, L., & Yang, B. (2020). Modification of structural, physicochemical and digestive properties of normal maize starch by thermal treatment. *Food Chemistry*, *309*, 125733.